

Towards stability results for global radial basis function based quadrature formulas*

Jan Glaubitz[†] and Jonah Reeger[‡]

Abstract. Quadrature formulas (QFs) based on radial basis functions (RBFs) have become an essential tool for multivariate numerical integration of scattered data. Although numerous works have been published on RBF-QFs, their stability theory can still be considered as underdeveloped. Here, we strive to pave the way towards a more mature stability theory for global and function-independent RBF-QFs. In particular, we prove stability of these for compactly supported RBFs under certain conditions on the shape parameter and the data points. As an alternative to changing the shape parameter, we demonstrate how the least-squares approach can be used to construct stable RBF-QFs by allowing the number of data points used for numerical integration to be larger than the number of centers used to generate the RBF approximation space. Moreover, it is shown that asymptotic stability of many global RBF-QFs is independent of polynomial terms, which are often included in RBF approximations. While our findings provide some novel conditions for stability of global RBF-QFs, the present work also demonstrates that there are still many gaps to fill in future investigations.

Key words. Numerical integration, radial basis functions, stability, cardinal functions, discrete orthogonal polynomials

AMS subject classifications (2020). 65D30, 65D32, 65D05, 42C05

1. Introduction. Numerical integration is an omnipresent task in mathematics and myriad applications. While these are too numerous to list fully, prominent examples include numerical differential equations [46, 76, 1], machine learning [68], finance [34], and biology [62]. In many cases, the problem can be formulated as follows. Let $\Omega \subset \mathbb{R}^D$ be a bounded domain with positive volume, $|\Omega| > 0$. Given N distinct data pairs $\{(\mathbf{x}_n, f_n)\}_{n=1}^N \subset \Omega \times \mathbb{R}$ with $f : \Omega \rightarrow \mathbb{R}$ and $f_n := f(\mathbf{x}_n)$, the aim is to approximate the weighted integral

$$I[f] := \int_{\Omega} f(\mathbf{x})\omega(\mathbf{x}) \, d\mathbf{x}$$

by an N -point QF. That is, by a weighted finite sum over the given function of the form

$$C_N[f] = \sum_{n=1}^N w_n f(\mathbf{x}_n).$$

In higher dimensions, C_N is sometimes referred to as an N -point cubature formula. The distinct points $\{\mathbf{x}_n\}_{n=1}^N$ are called *data points* and the $\{w_n\}_{n=1}^N$ are referred to as *quadrature weights*. Many QFs are derived based on the idea to approximate the (unknown) function f and then exactly integrate this approximation [43, 88, 25, 18, 57, 19, 58, 21, 9, 91]. Arguably, most of the existing QFs have been derived from being exact for polynomials up to a certain degree. See [63, 69, 20, 70, 19, 93], in addition to the above references.

That said, in recent years, QFs based on the exact integration of RBFs have received a growing amount of interest [87, 85, 84, 75, 2, 32, 78, 80, 95, 79, 86]. The increased use of RBFs for numerical

* January 31, 2023

Corresponding author: Jan Glaubitz (Jan.Glaubitz@Dartmouth.edu, orcid.org/0000-0002-3434-5563)

Disclaimer: The views expressed in this academic research paper are those of the authors and do not reflect the official policy or position of the United States Government or Department of Defense. In accordance with the Air Force Instruction 51-303, it is not copyrighted, but is the property of the United States government.

[†] Department of Mathematics, Dartmouth College, Hanover, NH 03755, USA

[‡] Air Force Institute of Technology, Wright–Patterson Air Force Base, OH 45433, USA.

integration and numerical differential equations [55, 53, 26, 54, 60, 51, 83, 31, 28, 39, 40] seems to be only logical, considering their story of success in the last few decades. In fact, since their introduction in Hardy’s work on cartography from 1971 (see [45]), RBFs have become a powerful tool in numerical analysis, including multivariate interpolation and approximation theory [12, 13, 98, 27, 52, 30]. It should also be mentioned that RBF-QF can be connected to (statistical) Bayesian quadrature [72, 67, 10, 56]. Finally, recent literature in the quadrature area [78, 80, 79, 77] has focused on ‘local’ RBF-FD-type implementations to reduce computational costs for large node numbers. While an extension to such local approaches would be of interest, we restrict ourselves to global RBF methods in this work. That said, to reduce the cost of constructing and integrating a global interpolant, a piecewise RBF interpolant could be considered and integrated in a manner similar to the construction of Newton–Cotes formulas. Some of our results would easily carry over to this setting, which might be seen as an extreme version (no overlap of nonzero measure) of RBF partition of unity methods [3, 97, 27] or the overlapped RBF-FD methods [82].

Even though RBF-QFs have been proposed and applied in numerous works, their stability theory can still be considered as under-developed, especially compared to more traditional—e.g. polynomial based—methods. Stability of RBF-QFs was broached, for instance, in [87, 85, 75]. Further, stability of RBF-QF was discussed in [32] for integration on certain manifolds. However, to the best of our knowledge, an exhaustive stability theory for RBF-QFs is still missing in the literature. In particular, theoretical results providing clear conditions under which stability of RBF-QFs is ensured are rarely encountered, even for global RBF methods.

The present work strives to fill this gap in the RBF literature partially. This is done by providing a detailed theoretical and numerical investigation on stability of global RBF-QFs¹ for different families of kernels, including compactly supported and Gaussian RBFs as well as polyharmonic splines (PHS). Our analysis resembles classic stability theory for quadratures exact for polynomial spaces. In contrast to some existing works (see [15] and references therein), we consider RBF approximations with function-independent shape parameters to obtain quadrature formulas that do not have to be recomputed when another function is considered.

In particular, we report on the following findings. (1) We provide a sufficient condition for compactly supported RBFs to yield a provable stable RBF-QF (see Theorem 4.1 in §4). The result is independent of the degree of the polynomial term that is included in the global RBF interpolant and assumes the data points to come from an equidistributed (space-filling) sequence. (2) We demonstrate how the idea of least squares can be employed to construct provable stable RBF-QFs. (3) Asymptotic stability of pure RBF-QFs is connected to asymptotic stability of the same RBF-QF but augmented with polynomials of a fixed arbitrary degree. Essentially, we can show that for a sufficiently large number of data points, stability of RBF-QFs is independent of the presence of polynomials in the RBF interpolant.

The rest of this work is organized as follows. We collect some preliminaries on RBF interpolants and QFs in §2. In §3, a few initial comments on stability of (RBF-)QFs are offered. Next, §4 contains our main theoretical result regarding stability of RBF-QFs based on compactly supported kernels. §5 demonstrates how the concept of least squares can be used to construct provable stable RBF-QFs. Furthermore, it is proven in §6 that, under certain assumptions, asymptotic stability of RBF-QFs is independent of the polynomial terms included in the RBF interpolant. Numerical tests in §7 accompany the previous theoretical findings. Finally, concluding thoughts are offered in §8.

2. Preliminaries. We collect some preliminaries on RBF interpolants (§2.1) and RBF-QFs (§2.2).

¹Henceforth, we will refer to these as “RBF-QFs”.

2.1. Radial basis function interpolation. RBFs are often considered a powerful tool in numerical analysis, including multivariate interpolation and approximation theory [12, 13, 98, 27, 52, 30]. We are especially interested in RBF interpolants. Let $f : \mathbb{R}^D \supset \Omega \rightarrow \mathbb{R}$ be a scalar valued function. Given a set of distinct *data points* (sometimes also referred to as *centers*), the *RBF interpolant* of f is of the form

$$(2.1) \quad (s_{N,d}f)(\mathbf{x}) = \sum_{n=1}^N \alpha_n \varphi(\varepsilon_n \|\mathbf{x} - \mathbf{x}_n\|_2) + \sum_{k=1}^K \beta_k p_k(\mathbf{x}).$$

Here, $\varphi : \mathbb{R}_0^+ \rightarrow \mathbb{R}$ is the *RBF* (also called *kernel*), $\{p_k\}_{k=1}^K$ is a basis of the space of algebraic polynomials up to degree d , $\mathbb{P}_d(\Omega)$, and the ε_n 's are nonnegative shape parameters.² The RBF interpolant (2.1) is uniquely determined by the conditions

$$(2.2) \quad (s_{N,d}f)(\mathbf{x}_n) = f(\mathbf{x}_n), \quad n = 1, \dots, N,$$

$$(2.3) \quad \sum_{n=1}^N \alpha_n p_k(\mathbf{x}_n) = 0, \quad k = 1, \dots, K.$$

Note that (2.2) and (2.3) can be reformulated as a linear system for the coefficient vectors $\boldsymbol{\alpha} = [\alpha_1, \dots, \alpha_N]^T$ and $\boldsymbol{\beta} = [\beta_1, \dots, \beta_K]^T$. This linear system is given by

$$(2.4) \quad \begin{bmatrix} \Phi & P \\ P^T & 0 \end{bmatrix} \begin{bmatrix} \boldsymbol{\alpha} \\ \boldsymbol{\beta} \end{bmatrix} = \begin{bmatrix} \mathbf{f} \\ \mathbf{0} \end{bmatrix},$$

where $\mathbf{f} = [f(\mathbf{x}_1), \dots, f(\mathbf{x}_N)]^T$ as well as

$$(2.5) \quad \Phi = \begin{bmatrix} \varphi(\varepsilon_1 \|\mathbf{x}_1 - \mathbf{x}_1\|_2) & \dots & \varphi(\varepsilon_N \|\mathbf{x}_1 - \mathbf{x}_N\|_2) \\ \vdots & & \vdots \\ \varphi(\varepsilon_1 \|\mathbf{x}_N - \mathbf{x}_1\|_2) & \dots & \varphi(\varepsilon_N \|\mathbf{x}_N - \mathbf{x}_N\|_2) \end{bmatrix}, \quad P = \begin{bmatrix} p_1(\mathbf{x}_1) & \dots & p_K(\mathbf{x}_1) \\ \vdots & & \vdots \\ p_1(\mathbf{x}_N) & \dots & p_K(\mathbf{x}_N) \end{bmatrix}.$$

For a constant shape parameter $\varepsilon_1 = \dots = \varepsilon_N$, (2.4) is ensured to have a unique solution—corresponding to existence and uniqueness of the RBF interpolant—if the kernel φ is conditionally positive definite of order d and the set of data points is $\mathbb{P}_d(\Omega)$ -unisolvent. See, for instance, [27, Chapter 7] and [35, Chapter 3.1] or references therein. In this work, we shall focus on the popular choices of RBFs listed in Table 1. A more complete list of RBFs and their properties can be found in the monographs [13, 98, 27, 30] and references therein.

The set of all RBF interpolants (2.1) forms an N -dimensional linear space, denote by $\mathcal{S}_{N,d}$. This space is spanned by the *cardinal functions*

$$(2.6) \quad c_m(\mathbf{x}) = \sum_{n=1}^N \alpha_n^{(m)} \varphi(\varepsilon_n \|\mathbf{x} - \mathbf{x}_n\|_2) + \sum_{k=1}^K \beta_k^{(m)} p_k(\mathbf{x}), \quad m = 1, \dots, N,$$

which are uniquely determined by the *cardinal property*

$$(2.7) \quad c_m(\mathbf{x}_n) = \delta_{mn} := \begin{cases} 1 & \text{if } m = n, \\ 0 & \text{otherwise,} \end{cases} \quad m, n = 1, \dots, N,$$

²For polyharmonic splines, it is common practice to not include a shape parameter in (2.1). For simplicity, we still use (2.1) and set $\varepsilon_n = 1$, $n = 1, \dots, n$, in this case.

| RBF | $\varphi(r)$ | parameter | order |
|----------------------|-------------------------------|-------------------------|---------|
| Gaussian | $\exp(-r^2)$ | | 0 |
| Wendland's | $\varphi_{D,k}(r)$, see [96] | $D, k \in \mathbb{N}_0$ | 0 |
| Polyharmonic splines | r^{2k-1} | $k \in \mathbb{N}$ | k |
| | $r^{2k} \log r$ | $k \in \mathbb{N}$ | $k + 1$ |

Table 1: Some popular RBFs. The “order” k of an RBF refers to the RBF being conditionally positive of order k .

and condition (2.3). They provide us with the following representation of the RBF interpolant (2.1):

$$(s_{N,df})(\mathbf{x}) = \sum_{n=1}^N f(\mathbf{x}_n) c_n(\mathbf{x})$$

This representation is convenient to subsequently derive quadrature weights based on RBFs that are independent of the function f .

2.2. Quadrature formulas based on radial basis functions. A fundamental idea behind many QFs is to first approximate the (unknown) function $f : \Omega \rightarrow \mathbb{R}$ based on the given data pairs $\{\mathbf{x}_n, f_n\}_{n=1}^N \subset \Omega \times \mathbb{R}$ and to exactly integrate this approximation. In the case of RBF-QFs this approximation is chosen as the RBF interpolant (2.1). Hence, the corresponding RBF-QF is defined as

$$(2.8) \quad C_N[f] := I[s_{N,df}] = \int_{\Omega} (s_{N,df})(\mathbf{x}) \omega(\mathbf{x}) d\mathbf{x}.$$

When formulated w. r. t. the cardinal functions c_n we get

$$(2.9) \quad C_N[f] = \sum_{n=1}^N w_n f(x_n) \quad \text{with} \quad w_n = I[c_n].$$

That is, the RBF quadrature weights $\mathbf{w} = [w_1, \dots, w_N]^T$ are given by the moments corresponding to the cardinal functions. This formulation is often preferred over (2.8) since the weights \mathbf{w} do not have to be recomputed when another function is considered. In our implementation, we compute the RBF quadrature weights by solving the linear system

$$(2.10) \quad \underbrace{\begin{bmatrix} \Phi & P \\ P^T & 0 \end{bmatrix}}_{=A} \begin{bmatrix} \mathbf{w} \\ \mathbf{v} \end{bmatrix} = \begin{bmatrix} \mathbf{m}^{\text{RBF}} \\ \mathbf{m}^{\text{poly}} \end{bmatrix},$$

where $\mathbf{v} \in \mathbb{R}^K$ is a Lagrange multiplier³. Furthermore, the vectors $\mathbf{m}^{\text{RBF}} \in \mathbb{R}^N$ and $\mathbf{m}^{\text{poly}} \in \mathbb{R}^K$ respectively contain the moments of the translated kernels and polynomial basis functions:

$$\begin{aligned} \mathbf{m}^{\text{RBF}} &= [I[\varphi_1], \dots, I[\varphi_N]]^T, \\ \mathbf{m}^{\text{poly}} &= [I[p_1], \dots, I[p_K]]^T, \end{aligned}$$

³The solution of (2.10) can be interpreted as the solution of an equality constrained linear optimization problem [5], where \mathbf{v} plays the role of a Lagrange multiplier.

with $\varphi_n(\mathbf{x}) = \varphi(\varepsilon_n \|\mathbf{x} - \mathbf{x}_n\|_2)$. The moments of different RBFs can be found in the appendix A. The polynomial moments can be found in the literature, e. g., [37, Appendix A] and [29, 61].

3. Stability and the Lebesgue constant. This section addresses the stability of RBF interpolants and the corresponding RBF-QFs. In particular, we show that both can be estimated in terms of the Lebesgue constant. This was also observed in [32] for RBF-QFs on certain (compact) manifolds. That said, we also demonstrate that RBF-QFs often come with improved stability compared to RBF interpolation.

3.1. Stability of quadrature formulas. We shall start by addressing stability of RBF-QFs. To this end, let us denote the best approximation of f from $\mathcal{S}_{N,d}$ in the L^∞ -norm by \hat{s} . That is,

$$\hat{s} = \arg \min_{s \in \mathcal{S}_{N,d}} \|f - s\|_{L^\infty(\Omega)} \quad \text{with} \quad \|f - s\|_{L^\infty(\Omega)} = \sup_{\mathbf{x} \in \Omega} |f(\mathbf{x}) - s(\mathbf{x})|.$$

Note that this best approximation w. r. t. the L^∞ -norm is not necessarily equal to the RBF interpolant. Still, the following error bound holds for the RBF-QF (2.9), that corresponds to exactly integrating the RBF interpolant from $\mathcal{S}_{N,d}$:

$$(3.1) \quad |C_N[f] - I[f]| \leq (\|I\|_\infty + \|C_N\|_\infty) \inf_{s \in \mathcal{S}_{N,d}} \|f - s\|_{L^\infty(\Omega)}$$

Inequality (3.1) is commonly known as the Lebesgue inequality; see, e. g., [94] or [9, Theorem 3.1.1]. It is often encountered in polynomial interpolation [11, 49] but straightforwardly carries over to numerical integration. In this context, the operator norms $\|I\|_\infty$ and $\|C_N\|_\infty$ are respectively given by $\|I\|_\infty = I[1]$ and

$$\|C_N\|_\infty = \sum_{n=1}^N |w_n| = \sum_{n=1}^N |I[c_n]|.$$

Recall that the c_n 's are the cardinal functions (see §2.1). In fact, $\|C_N\|_\infty$ is a common stability measure for QFs. This is because the propagation of input errors, e. g., due to noise or rounding errors, can be bounded by $\|C_N\|_\infty$: Let $\tilde{f} : \Omega \rightarrow \mathbb{R}$ be a perturbed version of f , e. g. including noise or measurement errors, then

$$|C_N[f] - C_N[\tilde{f}]| \leq \|C_N\|_\infty \|f - \tilde{f}\|_{L^\infty}.$$

In other words, input errors are amplified at most by a factor that is equal to the operator norm $\|C_N\|_\infty$. At the same time, we have

$$\|C_N\|_\infty \geq C_N[1],$$

where equality holds if and only if all quadrature weights are nonnegative. Also, for this reason, the construction of QFs is mainly devoted to nonnegative QFs.

Definition 3.1 (Stability). *We call the RBF-QF C_N stable if $\|C_N\|_\infty = C_N[1]$. This is the case if and only if $I[c_n] \geq 0$ for all cardinal functions c_n , $n = 1, \dots, N$.*

It is also worth noting that $C_N[1] = \|I\|_\infty$ if the QF is exact for constants. For RBF-QFs, this is the case if at least constants are included in the underlying RBF interpolant ($d \geq 0$).

3.2. Stability of RBF approximations. We now demonstrate how stability of the RBF-QF C_N can be connected to stability of the corresponding RBF interpolant. Indeed, the stability measure $\|C_N\|_\infty$ can be bounded from above by

$$\|C_N\|_\infty \leq \|I\|_\infty \Lambda_N, \quad \text{with} \quad \Lambda_N := \sup_{\mathbf{x} \in \Omega} \sum_{n=1}^N |c_n(\mathbf{x})|.$$

Here, Λ_N is the Lebesgue constant corresponding to the recovery process $f \mapsto s_{N,d}f$ (RBF interpolation). Obviously, $\Lambda_N \geq 1$. Also note that if $1 \in \mathcal{S}_{N,d}$ (the RBF-QF is exact for constants), we observe

$$(3.2) \quad \|I\|_\infty \leq \|C_N\|_\infty \leq \|I\|_\infty \Lambda_N.$$

Hence, the RBF-QF is stable ($\|C_N\|_\infty = \|I\|_\infty$) if Λ_N is minimal ($\Lambda_N = 1$). We briefly note that the inequality $\|C_N\|_\infty \leq \|I\|_\infty \Lambda_N$ is sharp by considering the following example.

Example 3.2 ($\|C_N\|_\infty = \Lambda_N$). Let us consider the domain $\Omega = [0, 1]$ with $\omega \equiv 1$, which immediately implies $\|I\|_\infty = 1$. In [7] it was shown that for the linear PHS $\varphi(r) = r$ and data points $0 = x_1 < \dots < x_N = 1$ the corresponding cardinal functions c_m are simple hat functions. In particular, c_m is the ordinary ‘‘connect the dots’’ piecewise linear interpolant of the data pairs (x_n, δ_{nm}) , $n = 1, \dots, N$. Thus, $\Lambda_N = 1$. At the same time, this yields $\|C_N\|_\infty = 1$ and therefore $\|C_N\|_\infty = \Lambda_N$.

Looking for minimal Lebesgue constants is a classical problem in approximation and recovery theory [65, 92]. For instance, it is well known that for polynomial interpolation, even near-optimal sets of data points yield a Lebesgue constant that grows as $\mathcal{O}(\log N)$ in one dimension and as $\mathcal{O}(\log^2 N)$ in two dimensions; see [11, 6, 8, 49]. In the case of RBF interpolation, the Lebesgue constant and appropriate data point distributions were studied, for instance, in [50, 22, 64, 23]. That said, the second inequality in (3.2) also tells us that in some cases, we can expect the RBF-QF to have superior stability properties compared to the underlying RBF interpolant. Finally, it should be stressed that (3.2) only holds if $1 \in \mathcal{S}_{N,d}$. In general, we have

$$C_N[1] \leq \|C_N\|_\infty \leq \|I\|_\infty \Lambda_N.$$

Still, this indicates that a recovery space $\mathcal{S}_{N,d}$ is desired that yields a small Lebesgue constant as well as the RBF-QF potentially having superior stability compared to RBF interpolation.

4. Compactly supported radial basis functions. Despite the increased use of RBF-QFs in applications, provable stability results are rarely encountered in the literature. As a first step towards a more mature stability theory, we next prove stability of RBF-QFs for compactly supported kernels with nonoverlapping supports. To be more precise, we subsequently consider RBFs $\varphi : \mathbb{R}_0^+ \rightarrow \mathbb{R}$ satisfying the following restrictions:

- (R1) φ is nonnegative, i. e., $\varphi \geq 0$.
- (R2) φ is uniformly bounded. W.l.o.g. we assume $\max_{r \in \mathbb{R}_0^+} |\varphi(r)| = 1$.
- (R3) φ is compactly supported. W.l.o.g. we assume $\text{supp } \varphi = [0, 1]$.

Already note that (R3) implies $\text{supp } \varphi_n = B_{\varepsilon_n^{-1}}(\mathbf{x}_n)$, where

$$B_{\varepsilon_n^{-1}}(\mathbf{x}_n) := \{ \mathbf{x} \in \Omega \mid \|\mathbf{x}_n - \mathbf{x}\|_2 \leq \varepsilon_n^{-1} \}, \quad \varphi_n(\mathbf{x}) := \varphi(\varepsilon_n \|\mathbf{x}_n - \mathbf{x}\|_2).$$

The φ_n 's will have nonoverlapping support if the shape parameters ε_n are sufficiently large. This can be ensured by the following condition:

$$(4.1) \quad \varepsilon_n^{-1} \leq h_n := \min \{ \|\mathbf{x}_n - \mathbf{x}_m\|_2 \mid \mathbf{x}_m \in X \setminus \{\mathbf{x}_n\} \}, \quad n = 1, \dots, N$$

Here, X denotes the set of data points. Finally, it should be pointed out that throughout this section, we assume $\omega \equiv 1$. This assumption is made for the main result, Theorem 4.1, to hold. Its role will become clearer after consulting the proof of Theorem 4.1 and is revisited in Remark 4.8.

4.1. Main result. Our main result is the following Theorem 4.1. After collecting a few preliminary results, its proof is given in §4.4.

Theorem 4.1. *Let $(\mathbf{x}_n)_{n \in \mathbb{N}}$ be an equidistributed sequence in Ω and $X_N = \{\mathbf{x}_n\}_{n=1}^N$. Furthermore, let $\omega \equiv 1$, let $\varphi : \mathbb{R}_0^+ \rightarrow \mathbb{R}$ be a RBF satisfying (R1) to (R3), and choose the shape parameters ε_n such that the corresponding functions φ_n have nonoverlapping support and equal moments ($I[\varphi_n] = I[\varphi_m]$ for all $n, m = 1, \dots, N$). For every polynomial degree $d \in \mathbb{N}$ there exists an $N_0 \in \mathbb{N}$ such that for all $N \geq N_0$ the corresponding RBF-QF (2.9) is stable. That is, $I[c_m] \geq 0$ for all $m = 1, \dots, N$.*

Note that a sequence $(\mathbf{x}_n)_{n \in \mathbb{N}}$ is equidistributed in Ω if and only if

$$\lim_{N \rightarrow \infty} \frac{|\Omega|}{N} \sum_{n=1}^N g(\mathbf{x}_n) = \int_{\Omega} g(\mathbf{x}) \, d\mathbf{x}$$

holds for all measurable bounded functions $g : \Omega \rightarrow \mathbb{R}$ that are continuous almost everywhere (in the sense of Lebesgue), see [99]. For details on equidistributed sequences, we refer to the monograph [59].⁴ Still, it should be noted that equidistributed sequences are dense sequences with a special ordering. In particular, if $(\mathbf{x}_n)_{n \in \mathbb{N}} \subset \Omega$ is equidistributed, then for every $d \in \mathbb{N}$ there exists an $N_0 \in \mathbb{N}$ such that X_N is $\mathbb{P}_d(\Omega)$ -unisolvent for all $N \geq N_0$; see [38]. This ensures that the corresponding RBF interpolant is well-defined. It should also be noted that if $\Omega \subset \mathbb{R}^D$ is bounded and has a boundary of measure zero (again in the sense of Lebesgue), then an equidistributed sequence in Ω is induced by an equidistributed sequence in the D -dimensional hypercube. More details on how an equidistributed sequence in Ω can be constructed are provided in [38].

Remark 4.2. It is always possible to ensure the equal moment condition, $I[\varphi_n] = I[\varphi_m]$ for all $n, m = 1, \dots, N$, in Theorem 4.1 by allowing the points closer to the boundary to come with a smaller shape parameter. In this way, one can compensate for the part of the support cut off by the boundary of the domain Ω . For instance, if equally spaced points are used on $[a, b]$ with $a = x_1 < \dots < x_N = b$, then the shape parameter is $\varepsilon_n = \varepsilon$ for the interior points ($n = 2, \dots, N - 1$) and $\varepsilon_1 = \varepsilon_N = \varepsilon/2$ for the boundary points, where ε is a suitable chosen reference parameter. That said, in our numerical tests, we observed Theorem 4.1 also to hold when the equal moment condition was not satisfied.

Remark 4.3. It is not necessary to include polynomials in the RBF-QF (2.9) for Theorem 4.1 to imply stability. Indeed, it is subsequently proved by Lemma 4.5 that the RBF-QF (2.9) can also be stable when no polynomials are included. Sometimes, the RBF-QF (2.9) is also referred to as the ‘‘RBF+poly-QF’’ when polynomials are included. In this regard, Theorem 4.1 shows that stability of RBF-QFs carries over to RBF+poly-QFs under the assumptions listed in Theorem 4.1. The influence of including polynomials into the RBF-QFs on their stability is also discussed for other kernels in §6.

4.2. Explicit representation of the cardinal functions. In preparation of proving Theorem 4.1 we derive an explicit representation for the cardinal functions c_n under the restrictions (R1)–(R3) and (4.1). In particular, we use the concept of discrete orthogonal polynomials (DOPs). Let us define the

⁴Examples for equidistributed sequences include low-discrepancy points [47, 71, 14, 24] used in quasi-Monte Carlo methods, such as the Halton points [44].

following discrete inner product corresponding to the data points $X_N = \{\mathbf{x}_n\}_{n=1}^N$:

$$(4.2) \quad [u, v]_{X_N} = \frac{|\Omega|}{N} \sum_{n=1}^N u(\mathbf{x}_n)v(\mathbf{x}_n)$$

Recall that the data points X_N are coming from an equidistributed sequence and are ensured to be $\mathbb{P}_d(\Omega)$ -unisolvent for any degree $d \in \mathbb{N}$ if N is sufficiently large. In this case, (4.2) is positive definite on $\mathbb{P}_d(\Omega)$, i. e., $[u, u]_{X_N} > 0$ if $u \in \mathbb{P}_d(\Omega)$ and $u \neq 0$. We say that the basis $\{p_k\}_{k=1}^K$ of $\mathbb{P}_d(\Omega)$, where $K = \dim \mathbb{P}_d(\Omega)$, consists of *DOPs* if

$$[p_k, p_l]_{X_N} = \delta_{kl} := \begin{cases} 1 & \text{if } k = l, \\ 0 & \text{otherwise,} \end{cases} \quad k, l = 1, \dots, K.$$

We now come to the desired explicit representation for the cardinal functions c_m .

Lemma 4.4 (Explicit representation for c_m). *Let the RBF $\varphi : \mathbb{R}_0^+ \rightarrow \mathbb{R}$ satisfy (R2) and (R3). Furthermore, choose the shape parameters ε_n such that the corresponding functions φ_n have nonoverlapping support and let the basis $\{p_k\}_{k=1}^K$ consists of DOPs. Then, the cardinal function c_m , $m = 1, \dots, N$, is given by*

$$(4.3) \quad c_m(\mathbf{x}) = \varphi_m(\mathbf{x}) - \frac{|\Omega|}{N} \sum_{n=1}^N \left(\sum_{k=1}^K p_k(\mathbf{x}_m)p_k(\mathbf{x}_n) \right) \varphi_n(\mathbf{x}) + \frac{|\Omega|}{N} \sum_{k=1}^K p_k(\mathbf{x}_m)p_k(\mathbf{x}).$$

Proof. Let $m, n \in \{1, \dots, N\}$. The restrictions (R2), (R3) together with the assumption of the φ_n 's having nonoverlapping support yields $\varphi_n(\mathbf{x}_m) = \delta_{mn}$. Hence, (2.6) and (2.7) imply

$$(4.4) \quad \alpha_n^{(m)} = \delta_{mn} - \sum_{k=1}^K \beta_k^{(m)} p_k(\mathbf{x}_n).$$

If we substitute (4.4) into (2.3), we get

$$p_l(\mathbf{x}_m) - \frac{N}{|\Omega|} \sum_{k=1}^K \beta_k^{(m)} [p_k, p_l]_{X_N} = 0, \quad l = 1, \dots, K.$$

Thus, if $\{p_k\}_{k=1}^K$ consists of DOPs, this gives us

$$(4.5) \quad \beta_l^{(m)} = \frac{N}{|\Omega|} p_l(\mathbf{x}_m), \quad l = 1, \dots, K.$$

Finally, substituting (4.5) into (4.4) yields

$$\alpha_n^{(m)} = \delta_{mn} - \frac{N}{|\Omega|} \sum_{k=1}^K p_k(\mathbf{x}_m)p_k(\mathbf{x}_n),$$

and therefore the assertion. ■

It should be stressed that using a basis of DOPs is not necessary for implementing RBF-QFs. In fact, the quadrature weights are—ignoring computational considerations— independent of the polynomial basis w. r. t. which the matrix P and the corresponding moments \mathbf{m}^{poly} are formulated. We only use DOPs as a theoretical tool to show stability of RBF-QFs.

4.3. Some low hanging fruits. Using the explicit representation (4.3) it is trivial to prove stability of RBF-QFs ($I[c_m] \geq 0$ for all $m = 1, \dots, N$) when no polynomial term or only a constant is included in the RBF interpolant.

Lemma 4.5 (No polynomials). *Let the RBF $\varphi : \mathbb{R}_0^+ \rightarrow \mathbb{R}$ satisfy (R1) to (R3) and choose the shape parameters ε_n such that the corresponding functions φ_n have nonoverlapping support. Assume that no polynomials are included in the corresponding RBF interpolant ($K = 0$). Then, the associated RBF-QF is stable.*

Proof. It is obvious that $c_m(\mathbf{x}) = \varphi_m(\mathbf{x})$. Thus, by restriction (R1), c_m is nonnegative and therefore $I[c_m] \geq 0$. ■

Lemma 4.6 (Only a constant). *Let the RBF $\varphi : \mathbb{R}_0^+ \rightarrow \mathbb{R}$ satisfy (R1) to (R3) and choose the shape parameters ε_n such that the corresponding functions φ_n have nonoverlapping support. Assume that only a constant is included in the corresponding RBF interpolant ($K = 1$). Then, the associated RBF-QF is stable.*

Proof. Let $m \in \{1, \dots, N\}$. If we choose $p_1 \equiv |\Omega|^{-1/2}$, Lemma 4.4 yields

$$c_m(\mathbf{x}) = \varphi_m(\mathbf{x}) + \frac{1}{N} \left(1 - \sum_{n=1}^N \varphi_n(\mathbf{x}) \right).$$

Note that by (R2), (R3), and (4.1), we therefore have $c_m(\mathbf{x}) \geq \varphi_m(\mathbf{x})$. Hence, (R1) implies the assertion. ■

4.4. Proof of the main results. The following technical Lemma will be convenient to the proof of Theorem 4.1.

Lemma 4.7. *Let $(\mathbf{x}_n)_{n \in \mathbb{N}}$ be equidistributed in Ω , $X_N = \{\mathbf{x}_n\}_{n=1}^N$, and let $[\cdot, \cdot]_{X_N}$ be the discrete inner product (4.2). Furthermore, let $\{p_k^{(N)}\}_{k=1}^K$ be a basis of $\mathbb{P}_d(\Omega)$ consisting of DOPs w. r. t. $[\cdot, \cdot]_{X_N}$. Then, for all $k = 1, \dots, K$,*

$$p_k^{(N)} \rightarrow p_k \quad \text{in } L^\infty(\Omega), \quad N \rightarrow \infty,$$

where $\{p_k\}_{k=1}^K$ is a basis of $\mathbb{P}_d(\Omega)$ consisting of continuous orthogonal polynomials satisfying

$$\int_{\Omega} p_k(\mathbf{x}) p_l(\mathbf{x}) \, d\mathbf{x} = \delta_{kl}, \quad k, l = 1, \dots, K.$$

Moreover, it holds that

$$\lim_{N \rightarrow \infty} \int_{\Omega} p_k^{(N)}(\mathbf{x}) p_l^{(N)}(\mathbf{x}) \, d\mathbf{x} = \delta_{kl}, \quad k, l = 1, \dots, K.$$

Proof. The assertion is a combination of Lemma 11 and 12 from [37], where a general positive weight function ω was considered. Here, we only consider the case $\omega \equiv 1$. ■

Essentially, Lemma 4.7 states that if a sequence of discrete inner products converges to a continuous one, then also the corresponding DOPs—assuming that the ordering of the elements does not change—converges to a basis of continuous orthogonal polynomials. Furthermore, this convergence holds in a uniform sense. We are now able to provide a proof for Theorem 4.1.

Proof of Theorem 4.1. Let $d \in \mathbb{N}$ and $m \in \{1, \dots, N\}$. Under the assumptions of Theorem 4.1, we have $I[\varphi_n] = I[\varphi_m]$ for all $n = 1, \dots, N$. Thus, Lemma 4.4 implies

$$I[c_m] = I[\varphi_m] \left(1 - \frac{|\Omega|}{N} \sum_{n=1}^N \sum_{k=1}^K p_k^{(N)}(\mathbf{x}_m) p_k^{(N)}(\mathbf{x}_n) \right) + \frac{|\Omega|}{N} \sum_{k=1}^K p_k^{(N)}(\mathbf{x}_m) I[p_k].$$

Let $\{p_k^{(N)}\}_{k=1}^K$ be a basis of $\mathbb{P}_d(\Omega)$ consisting of DOPs. That is, $[p_k^{(N)}, p_l^{(N)}]_{X_N} = \delta_{kl}$. In particular, $p_1^{(N)} \equiv |\Omega|^{-1/2}$. With this in mind, it is easy to verify that

$$(4.6) \quad \frac{|\Omega|}{N} \sum_{n=1}^N \sum_{k=1}^K p_k^{(N)}(\mathbf{x}_m) p_k^{(N)}(\mathbf{x}_n) = \sum_{k=1}^K p_k^{(N)}(\mathbf{x}_m) |\Omega|^{1/2} [p_k^{(N)}, p_1^{(N)}]_{X_N} = 1.$$

Thus, we have

$$I[c_m] \geq 0 \iff \sum_{k=1}^K p_k^{(N)}(\mathbf{x}_m) I[p_k^{(N)}] \geq 0.$$

Finally, observe that

$$\sum_{k=1}^K p_k^{(N)}(\mathbf{x}_m) I[p_k^{(N)}] = |\Omega|^{1/2} \sum_{k=1}^K p_k^{(N)}(\mathbf{x}_m) \int_{\Omega} p_k^{(N)}(\mathbf{x}) p_1^{(N)}(\mathbf{x}) d\mathbf{x},$$

under the assumption that $\omega \equiv 1$. Lemma 4.7 therefore implies

$$(4.7) \quad \lim_{N \rightarrow \infty} \sum_{k=1}^K p_k^{(N)}(\mathbf{x}_m) I[p_k^{(N)}] = 1,$$

which completes the proof. ■

Remark 4.8 (On the assumption that $\omega \equiv 1$). The assumption that $\omega \equiv 1$ in Theorem 4.1 is necessary for (4.6) and (4.7) to both hold true. On the one hand, (4.6) is ensured by the the DOPs being orthogonal w. r. t. the discrete inner product (4.2). This discrete inner product can be considered as an approximation to the continuous inner product $\langle u, v \rangle = \int_{\Omega} u(\mathbf{x}) v(\mathbf{x}) d\mathbf{x}$. This also results in Lemma 4.7. On the other hand, in general, (4.7) only holds if the DOPs converge to a basis of polynomials that is orthogonal w. r. t. the weighted continuous inner product $\langle u, v \rangle_{\omega} = \int_{\Omega} u(\mathbf{x}) v(\mathbf{x}) \omega(\mathbf{x}) d\mathbf{x}$. Hence, for (4.6) and (4.7) to both hold true at the same time, we have to assume that $\omega \equiv 1$. In this case, the two continuous inner products are the same.

5. Provable stable least squares RBF-QFs. Theorem 4.1 shows that compactly supported RBFs (e. g. Wendland's kernels) can lead to stable interpolatory QFs if the shape parameter is so that none of the shifted kernels have a region of overlap. In our numerical tests, we observed this condition not just to be sufficient but also often being "close to" necessary. We often found the RBF-QF even to have negative weights when the support regions only slightly overlapped. At the same time, it is known that scaling Wendland's kernels so that the support decreases with the number of data points results in the interpolation error to decrease only slowly or even to stagnate [27].

To provide a more practical procedure for ensuring stability of RBF-QFs, we now demonstrate how a least-squares approach [48, 42, 36, 37] can be used to construct stable RBF-QFs by allowing the

number of data points used for numerical integration to be larger than the number of centers that are used to generate the RBF approximation space. The subsequent least-squares approach is *not* limited to compactly supported kernels and can be used to construct stable QFs that are exact for fairly general RBF approximation spaces. The only restrictions are that the RBF approximation space consists of continuous and bounded functions and contains constants. Further, the number of data points used by quadrature has to be sufficiently larger than the dimension of the RBF approximation space. Although the least-squares approach has recently been extended to general multi-dimensional function spaces that include constants in [38], the implications for RBF-QF have not yet been explored. To this end, we consider a given center point set $Y_M = \{\mathbf{y}_m\}_{m=1}^M$, generating the M -dimensional RBF space $\mathcal{S}_{M,d}$, and a larger data point set $X_N = \{\mathbf{x}_n\}_{n=1}^N$ with $N > M$. Then, any QF $C_N[f] = \sum_{n=1}^N w_n f(x_n)$ that is exact for all $f \in \mathcal{S}_{M,d}$ has to satisfy

$$(5.1) \quad \underbrace{\begin{bmatrix} b_1(\mathbf{x}_1) & \dots & b_1(\mathbf{x}_N) \\ \vdots & & \vdots \\ b_M(\mathbf{x}_1) & \dots & b_M(\mathbf{x}_N) \end{bmatrix}}_{=B} \underbrace{\begin{bmatrix} w_1 \\ \vdots \\ w_N \end{bmatrix}}_{=\mathbf{w}} = \underbrace{\begin{bmatrix} I[b_1] \\ \vdots \\ I[b_M] \end{bmatrix}}_{=\mathbf{m}},$$

where $\{b_m\}_{m=1}^M$ is a basis of $\mathcal{S}_{M,d}$. The matrix B in (5.1) depends on X_N and Y_M (as well as on the kernel φ and the polynomial degree d), which we denote by $B = B(X_N, Y_M)$. Assume that the data point set X_N is $\mathcal{S}_{M,d}$ -unisolvent, i. e.,

$$f(\mathbf{x}_n) = 0, \forall \mathbf{x}_n \in X_N \implies f \equiv 0$$

holds for all $f \in \mathcal{S}_{M,d}$.⁵ Then (5.1) has infinitely many solutions, which form a $(N - M)$ -dimensional affine linear subspace W . Every $\mathbf{w} \in W$ yields a QF that is exact for all functions from the RBF space $\mathcal{S}_{M,d}$. We want to find a positive solution $\mathbf{w} \in W$ so that the corresponding QF with weights \mathbf{w} is stable (see Definition 3.1). To this end, we use the following result from [38].

Lemma 5.1 (Corollary 3.6 in [38]). *Let $\Omega \subset \mathbb{R}^D$, $\omega : \Omega \rightarrow \mathbb{R}_0^+$ be a Riemann integrable weight function that is positive almost everywhere, and let $\mathcal{F} = \text{span}\{b_m \mid m = 1, \dots, M\}$ be a finite-dimensional linear space of continuous and bounded functions that contains constants. Further, let $(\mathbf{x}_n)_{n \in \mathbb{N}}$ be an equidistributed sequence in Ω with $\omega(\mathbf{x}_n) > 0$ for all $n \in \mathbb{N}$ and denote the affine linear subspace of solutions of (5.1) by $W_{\mathcal{F}}$. Then there exists an $N_0 \in \mathbb{N}$ such that for all $N \geq N_0$ and discrete weights*

$$r_{n,N} = |\Omega|\omega(\mathbf{x}_n)/N, \quad n = 1, \dots, N,$$

the corresponding least-squares QF

$$C_N^{\text{LS}}[f] = \sum_{n=1}^N w_n^{\text{LS}} f(\mathbf{x}_n) \quad \text{with} \quad \mathbf{w}^{\text{LS}} = \arg \min_{\mathbf{w} \in W_{\mathcal{F}}} \|R^{-1/2} \mathbf{w}\|_2,$$

where $R^{-1/2} = \text{diag}(1/\sqrt{r_1}, \dots, 1/\sqrt{r_N})$, is positive and exact for all $f \in \mathcal{F}$.

If we apply Lemma 5.1 to the RBF function space $\mathcal{S}_{M,d}$, we get Corollary 5.2.

⁵ X_N is $\mathcal{S}_{M,d}$ -unisolvent, for instance, when the kernel φ is conditionally positive definite of order d and X_N is $\mathbb{P}_d(\Omega)$ -unisolvent, which is a common assumption to ensure uniqueness of RBF interpolants.

Corollary 5.2. *Let $\Omega \subset \mathbb{R}^D$ be compact and let $\omega : \Omega \rightarrow \mathbb{R}_0^+$ be a Riemann integrable weight function that is positive almost everywhere. Further, let $d \geq 0$ be an integer, let $\varphi : \mathbb{R}_0^+ \rightarrow \mathbb{R}$ be a continuous and conditionally positive kernel of order d , and let $\{\mathbf{y}_m\}_{m=1}^M$ be a given set of centers. If $(\mathbf{x}_n)_{n \in \mathbb{N}}$ is an equidistributed sequence in Ω with $\omega(\mathbf{x}_n) > 0$ for all $n \in \mathbb{N}$, then there exists an $N_0 \in \mathbb{N}$ such that for all $N \geq N_0$ and discrete weights*

$$r_{n,N} = |\Omega| \omega(\mathbf{x}_n) / N, \quad n = 1, \dots, N,$$

the corresponding least-squares RBF-QF

$$(5.2) \quad C_N^{\text{LS}}[f] = \sum_{n=1}^N w_n^{\text{LS}} f(\mathbf{x}_n) \quad \text{with} \quad \mathbf{w}^{\text{LS}} = \arg \min_{\mathbf{w} \in W} \|R^{-1/2} \mathbf{w}\|_2,$$

where $R^{-1/2} = \text{diag}(1/\sqrt{r_1}, \dots, 1/\sqrt{r_N})$, is positive and exact for all $f \in \mathcal{S}_{M,d}$.

Proof. We first note that the RBF function space $\mathcal{S}_{M,d}$, which we defined in §2, is M -dimensional with $M < \infty$, i. e., finite-dimensional. Because the kernel φ and all polynomials up to degree d are continuous, all functions from $\mathcal{S}_{M,d}$ are continuous. Further, since $\Omega \subset \mathbb{R}^D$ is compact and all functions from $\mathcal{S}_{M,d}$ are continuous, they are also bounded. Finally, $d \geq 0$ implies that $\mathcal{S}_{M,d}$ contains constants. Corollary 5.2 now follows from Lemma 5.1 with $\mathcal{F} = \mathcal{S}_{M,d}$. ■

The weighted least-squares solution (5.2) has the advantage of being easy and efficient to compute using standard tools from linear algebra. The above discussion motivates us to formulate the following procedure to construct stable least-squares RBF-QFs (LSRBF-QFs).

Algorithm 5.1 Constructing stable LSRBF-QFs

- 1: **Input:** Center points $\{\mathbf{y}_m\}_{m=1}^M$, kernel φ , polynomial degree $d \geq 0$, weight function ω , and equidistributed data points $(\mathbf{x}_n)_{n \in \mathbb{N}}$
 - 2: **Output:** An integer $N \geq M$ and a stable LSRBF-QF with points $\{\mathbf{x}_n\}_{n=1}^N$ and weights $\mathbf{w}^{\text{LS}} \in \mathbb{R}^N$
 - 3: Set \mathbf{w}^{LS} equal to the weights of the interpolatory RBF-QF given by (2.10)
 - 4: **repeat**
 - 5: Increase the number of data points by one: $N = N + 1$
 - 6: Set $X_N = \{\mathbf{x}_n\}_{n=1}^N$
 - 7: Compute the matrix $B = B(X_N, Y_M)$ as in (5.1)
 - 8: Compute the weighted least-squares solution \mathbf{w}^{LS} as in (5.2)
 - 9: Determine the smallest weight: $w_{\min} = \min(\mathbf{w}^{\text{LS}})$
 - 10: **until** $\mathbf{w}^{\text{LS}} \geq 0$
-

Algorithm 5.1 assumes that X_M is $\mathcal{S}_{M,d}$ -unisolvent, since the interpolatory RBF-QF given by (2.10) would not be defined otherwise. The possible advantage of stable LSRBF-QFs compared to (potentially unstable) interpolatory RBF-QFs is demonstrated in §7.2. Finally, we point out the potential application of stable LSRBF-QFs to the construction of stable RBF methods for time-dependent hyperbolic partial differential equations [90, 41]. A crucial part of these methods is replacing exact integrals involving the approximate solution—in this case, an (local) RBF function—with a quadrature that should be as accurate as possible for functions from the approximation space.

6. Polynomial terms do not influence asymptotic stability. Recall that Theorem 4.1 in §4 holds regardless of the degree d of the polynomial term included in the RBF interpolant. Indeed, one might generally ask, “how are polynomial terms influencing stability of the RBF-QF?”. In what follows, we

address this question by showing that—under certain assumptions that are to be specified yet—at least asymptotic stability of RBF-QFs is independent of polynomial terms.

Recently, the following explicit formula for the cardinal functions was derived in [5, 4]. Let us denote $\mathbf{c}(\mathbf{x}) = [c_1(\mathbf{x}), \dots, c_N(\mathbf{x})]^T$, where c_1, \dots, c_N are the cardinal functions spanning $\mathcal{S}_{N,d}$; see (2.6) and (2.7). Provided that Φ and P in (2.5) have full rank⁶,

$$(6.1) \quad \mathbf{c}(\mathbf{x}) = \hat{\mathbf{c}}(\mathbf{x}) - B\boldsymbol{\tau}(\mathbf{x})$$

holds. Here, $\hat{\mathbf{c}}(\mathbf{x}) = [\hat{c}_1(\mathbf{x}), \dots, \hat{c}_N(\mathbf{x})]^T$ are the cardinal functions corresponding to the pure RBF interpolation without polynomials. That is, they span $\mathcal{S}_{N,-1}$. At the same time, B and $\boldsymbol{\tau}$ are defined as

$$B := \Phi^{-1}P \left(P^T \Phi^{-1}P \right)^{-1}, \quad \boldsymbol{\tau}(\mathbf{x}) := P^T \hat{\mathbf{c}}(\mathbf{x}) - \mathbf{p}(\mathbf{x})$$

with $\mathbf{p}(\mathbf{x}) = [p_1(\mathbf{x}), \dots, p_K(\mathbf{x})]^T$. Note that $\boldsymbol{\tau}$ can be interpreted as a residual measuring how well pure RBFs can approximate polynomials up to degree d . Recalling (2.9), we see that (6.1) implies

$$(6.2) \quad \mathbf{w} = \hat{\mathbf{w}} - BI[\boldsymbol{\tau}],$$

where \mathbf{w} is the vector of quadrature weights of the RBF-QF with polynomials ($d \geq 0$). At the same time, $\hat{\mathbf{w}}$ is the vector of weights corresponding to the pure RBF-QF without polynomial augmentation ($d = -1$). Moreover, $I[\boldsymbol{\tau}]$ denotes the componentwise application of the integral operator I . It was numerically demonstrated in [5] that for fixed $d \in \mathbb{N}$ one has

$$(6.3) \quad \max_{\mathbf{x} \in \Omega} \|B\boldsymbol{\tau}(\mathbf{x})\|_{\ell^\infty} \rightarrow 0 \quad \text{as } N \rightarrow \infty$$

if PHS are used. Note that, for fixed $\mathbf{x} \in \Omega$, $B\boldsymbol{\tau}(\mathbf{x})$ is an N -dimensional vector and $\|B\boldsymbol{\tau}(\mathbf{x})\|_{\ell^\infty}$ denotes its ℓ^∞ -norm. That is, the maximum absolute value of the N components. It should be pointed out that (6.3) was numerically demonstrated only for PHS in [5]. However, the relations (6.1) and (6.2) hold for general RBFs as well as varying shape parameters, assuming that Φ and P have full rank. Please see [5, Section 4] for more details. We also remark that (6.3) implies the weaker statement

$$(6.4) \quad \|B\boldsymbol{\tau}(\cdot)\|_{\ell^1} \rightarrow 0 \quad \text{in } L^1(\Omega) \quad \text{as } N \rightarrow \infty.$$

Here, $B\boldsymbol{\tau}(\cdot)$ denotes a vector-valued function, $B\boldsymbol{\tau} : \Omega \rightarrow \mathbb{R}^N$. That is, for a fixed argument $\mathbf{x} \in \Omega$, $B\boldsymbol{\tau}(\mathbf{x})$ is an N -dimensional vector in \mathbb{R}^N and $\|B\boldsymbol{\tau}(\mathbf{x})\|_{\ell^1}$ denotes the usual ℓ^1 -norm of this vector. Thus, (6.4) means that the integral of the ℓ^1 -norm of the vector-valued function $B\boldsymbol{\tau}(\cdot)$ converges to zero as $N \rightarrow \infty$. The above condition is not just weaker than (6.3) (see Remark 6.4), but also more convenient to investigate stability of QFs. Indeed, we have the following results.

Theorem 6.1. *Let $\omega \in L^\infty(\Omega)$. Assume Φ and P in (2.5) have full rank, and assume (6.4) holds. Then the two following statements are equivalent:*

- (a) $\|\hat{\mathbf{w}}\|_{\ell^1} \rightarrow \|I\|_\infty$ for $N \rightarrow \infty$
- (b) $\|\mathbf{w}\|_{\ell^1} \rightarrow \|I\|_\infty$ for $N \rightarrow \infty$

That is, either both the pure and polynomial augmented RBF-QF are asymptotically stable or none is.

A short discussion on the term ‘‘asymptotically stable’’ is subsequently provided in Remark 6.2.

⁶ P having full rank means that P has full column rank, i.e., the columns of P are linearly independent. This is equivalent to the set of data points being $\mathbb{P}_d(\Omega)$ -unisolvant.

Proof. Assume Φ and P in (2.5) have full rank, and assume (6.4) holds. Then (6.2) follows and therefore

$$(6.5) \quad \begin{aligned} \|\mathbf{w}\|_{\ell^1} &\leq \|\hat{\mathbf{w}}\|_{\ell^1} + \|BI[\boldsymbol{\tau}]\|_{\ell^1}, \\ \|\hat{\mathbf{w}}\|_{\ell^1} &\leq \|\mathbf{w}\|_{\ell^1} + \|BI[\boldsymbol{\tau}]\|_{\ell^1}. \end{aligned}$$

Next, note that $BI[\boldsymbol{\tau}] = I[B\boldsymbol{\tau}]$, and thus

$$\|BI[\boldsymbol{\tau}]\|_{\ell^1} = \sum_{n=1}^N |I[(B\boldsymbol{\tau})_n]| \leq I \left[\sum_{n=1}^N |(B\boldsymbol{\tau})_n| \right] = I [\|B\boldsymbol{\tau}\|_{\ell^1}].$$

Since $\omega \in L^\infty(\Omega)$, it follows that

$$\|BI[\boldsymbol{\tau}]\|_{\ell^1} \leq \|\omega\|_{L^\infty(\Omega)} \int_{\Omega} \|B\boldsymbol{\tau}(\mathbf{x})\|_{\ell^1} d\mathbf{x}.$$

Hence, by assuming that (6.4) holds, we get $\|BI[\boldsymbol{\tau}]\|_{\ell^1} \rightarrow 0$ for fixed $d \in \mathbb{N}$ and $N \rightarrow \infty$. Finally, substituting this into (6.5) yields the assertion. \blacksquare

Theorem 6.1 states that—under the listed assumptions—it is sufficient to consider asymptotic stability of the pure RBF-QF. Once asymptotic (in)stability is established for the pure RBF-QF, by Theorem 6.1, it also carries over to all corresponding augmented RBF-QFs. Interestingly, this follows our findings for compactly supported RBFs reported in Theorem 4.1. There, conditional stability was ensured independently of the degree of the augmented polynomials.

Remark 6.2 (Asymptotic stability). We call a sequence of QFs with weights $\mathbf{w}_N \in \mathbb{R}^N$ for $N \in \mathbb{N}$ asymptotically stable if $\|\mathbf{w}_N\|_{\ell^1} \rightarrow \|I\|_\infty$ for $N \rightarrow \infty$. Recall that $\|\mathbf{w}_N\|_{\ell^1} = \|C_N\|_\infty$ if the weights \mathbf{w}_N correspond to the N -point QF C_N . It is easy to note that this is a weaker property than every single QF being stable, i. e., $\|\mathbf{w}_N\|_{\ell^1} = \|I\|_\infty$ for all $N \in \mathbb{N}$. That said, consulting (3.1), asymptotic stability is sufficient for the QF to converge for all functions that can be approximated arbitrarily accurate by RBFs w. r. t. the $L^\infty(\Omega)$ -norm. Of course, the propagation of input errors might be suboptimal for every single QF.

Theorem 6.1 makes two assumptions. (1) Φ and P are full rank matrices; and (2) the condition (6.3) holds. In the two following remarks, we comment on these assumptions.

Remark 6.3 (On the first assumption of Theorem 6.1). Although requiring A and P to have full rank might seem restrictive, there are often even more restrictive constraints in practical problems. For instance, when solving partial differential equations, the data points are usually required to be smoothly scattered so that the distance between data points is kept roughly constant. It seems unlikely to find A and P to be singular for such data points. See [5] for more details.

Remark 6.4 (On the second assumption of Theorem 6.1). The second assumption for Theorem 6.1 to hold is that (6.4) is satisfied. That is, the integral of $\|B\boldsymbol{\tau}(\cdot)\|_{\ell^1} : \Omega \rightarrow \mathbb{R}_0^+$ converges to zero as $N \rightarrow \infty$. This is a weaker condition than the maximum value of $\|B\boldsymbol{\tau}(\cdot)\|_{\ell^1}$ converging to zero, which was numerically observed to hold for PHS in [5]. The relation between these conditions can be observed by applying Hölder's inequality (see, for instance, [81, Chapter 3]). Let $1 \leq p, q \leq \infty$ with $1/p + 1/q = 1$ and assume that $\omega \in L^q(\Omega)$. Then we have

$$\int_{\Omega} \|B\boldsymbol{\tau}(\mathbf{x})\|_{\ell^1} \omega(\mathbf{x}) d\mathbf{x} \leq \left(\int_{\Omega} \|B\boldsymbol{\tau}(\mathbf{x})\|_{\ell^1}^p d\mathbf{x} \right)^{1/p} \left(\int_{\Omega} \omega(\mathbf{x})^q d\mathbf{x} \right)^{1/q}.$$

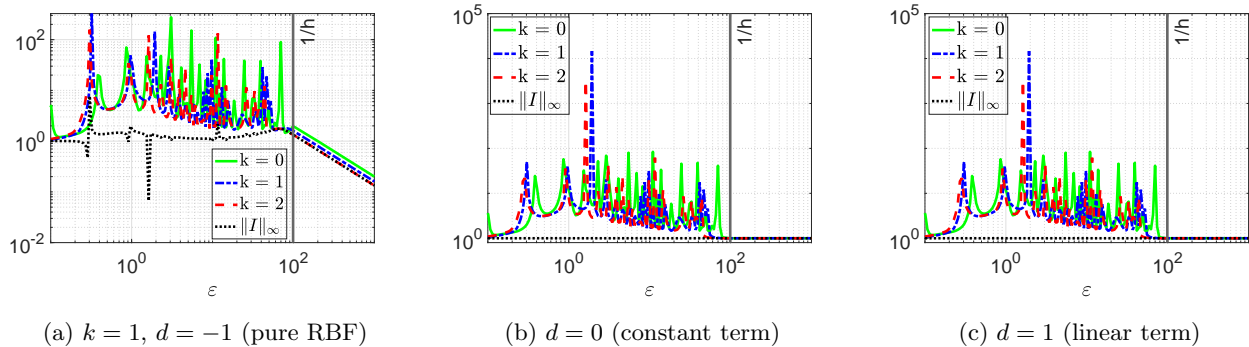


Figure 1: The stability measure $\|C_N\|_\infty$ for Wendland's compactly supported RBF $\varphi_{1,k}$ with smoothness parameters $k = 0, 1, 2$ on $N = 100$ equidistant data points. $1/h$ denotes the threshold above which the basis functions have nonoverlapping support.

Hence, $\|B\tau\|_{\ell^1}$ converging to zero in $L^p(\Omega)$ as $N \rightarrow \infty$ for some $p \geq 1$ immediately implies (6.2). The special case of $p = \infty$ corresponds to (6.3).

7. Numerical results. We present a variety of numerical tests in one and two dimensions to demonstrate our theoretical findings. A constant weight function $\omega \equiv 1$ is used for simplicity. All numerical tests presented here were generated in MATLAB⁷.

7.1. Compactly supported RBFs. Let us start with demonstrating Theorem 4.1 in one dimension. To this end, we consider Wendland's compactly supported RBFs in $\Omega = [0, 1]$.

Figure 1 illustrates the stability measure $\|C_N\|_\infty$ of Wendland's compactly supported RBF $\varphi_{1,k}$ with smoothness parameters $k = 0, 1, 2$ as well as the optimal stability measure. The latter is given by $C_N[1]$ if no constants are included and by $\|I\|_\infty = 1$ if constants are included in the RBF approximation space. Furthermore, $N = 100$ equidistant data points were used, including the end points, $x_1 = 0$ and $x_N = 1$, and the (reference) shape parameter ε was allowed to vary. Finally, $1/h$ denotes the threshold above which the compactly supported RBFs have nonoverlapping support. We note that the RBF-QFs are stable for sufficiently small shape parameters. At the same time, we can also observe the RBF-QF be stable for $\varepsilon \geq 1/h$. It can be argued that this is in accordance with Theorem 4.1. Recall that Theorem 4.1 essentially states that for $\varepsilon \geq 1/h$, and assuming that all basis functions have equal moments ($I[\varphi_n] = I[\varphi_m]$ for all n, m), the corresponding RBF-QF (including polynomials of any degree) is stable if a sufficiently large number of equidistributed data points is used. Here, the equal moments condition was ensured by choosing the shape parameter as $\varepsilon_n = \varepsilon$ for the interior data points ($n = 2, \dots, N - 1$) and as $\varepsilon_1 = \varepsilon_N = \varepsilon/2$ for the boundary data points.

That said, at least numerically, we observe that it is possible to drop this equal moment condition. This is demonstrated by Figure 2. There, we perform the same test as in Figure 1, except choosing all the shape parameters to be equal ($\varepsilon_n = \varepsilon, n = 1, \dots, N$) and going over to nonequidistant Halton points. Nevertheless, we can see in Figure 2 that for $\varepsilon \geq 1/h$ the RBF-QFs are still stable.

Next, we extend our numerical tests to the following Genz test functions [33] (also see [94]) on

⁷See https://github.com/jglaubitiz/stability_RBF_CFs

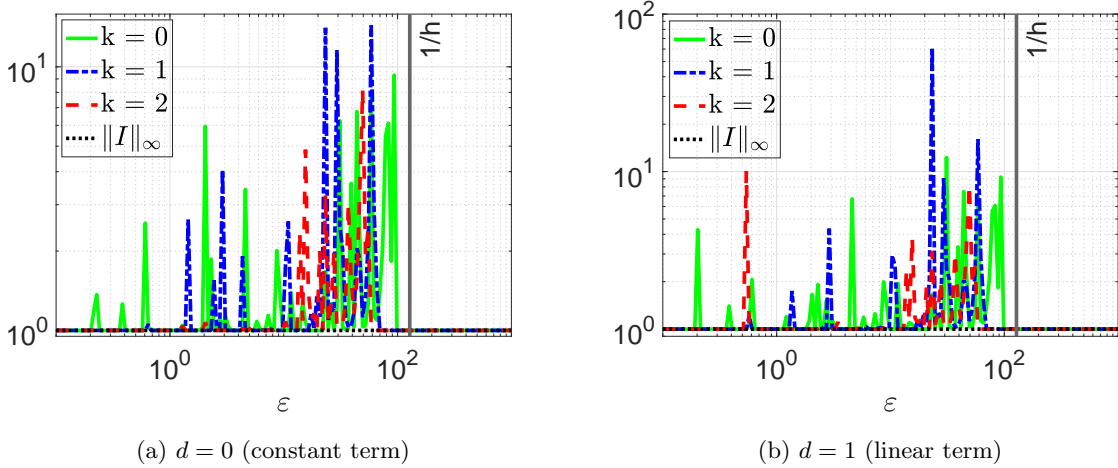


Figure 2: The stability measure $\|C_N\|_\infty$ for Wendland's compactly supported RBF $\varphi_{1,k}$ with smoothness parameters $k = 0, 1, 2$ on $N = 100$ Halton points. $1/h$ denotes the threshold above which the basis functions have nonoverlapping support.

$\Omega = [0, 1]^q$:

$$(7.1) \quad \begin{aligned} g_1(\mathbf{x}) &= \cos\left(2\pi b_1 + \sum_{i=1}^q a_i x_i\right), & g_2(\mathbf{x}) &= \prod_{i=1}^q \left(a_i^{-2} + (x_i - b_i)^2\right)^{-1}, \\ g_3(\mathbf{x}) &= \left(1 + \sum_{i=1}^q a_i x_i\right)^{-(q+1)}, & g_4(\mathbf{x}) &= \exp\left(-\sum_{i=1}^q a_i^2 (x_i - b_i)^2\right) \end{aligned}$$

Here, q denotes the dimension under consideration and is henceforth chosen as $q = 2$. These functions are designed to have different complex characteristics for numerical integration routines. The vectors $\mathbf{a} = (a_1, \dots, a_q)^T$ and $\mathbf{b} = (b_1, \dots, b_q)^T$ respectively contain (randomly chosen) shape and translation parameters. For each case, the experiment was repeated 100 times. At the same time, for each experiment, the vectors \mathbf{a} and \mathbf{b} were drawn randomly from $[0, 1]^2$. For reasons of space, we only report the results for g_1 and $k = 1$ in Figure 3. As before, the smallest errors are found for shape parameters corresponding to the stable RBF-QF. The results for g_2, g_3, g_4 and $k = 0, 2$ were similar and are therefore not reported here. Since it might be hard to identify the smallest errors as well as the corresponding shape parameter and stability measure from Figure 3, these are listed in Table 2 for $d = 0, 1$ together with the corresponding values for the fourth Genz test function g_4 .

We see in Figure 3 that for $d = -1$ and increasing ε , the error increases. This is because the supports of the translated kernels (disks in 2d) become smaller, resulting in “holes” in the pure RBF interpolant, i. e., regions where it is zero. In Figure 3c, for random points and $d = -1$, the supports become so small that all the quadrature weights become zero. The holes vanish if at least a constant is included in the RBF interpolant, which explains the reduced errors for the same value of ε when $d = 0$ or $d = 1$. Finally, even for nonoverlapping supports ($\varepsilon = 1/h$), the area of the holes in the pure RBF part of the interpolant can converge to zero⁸ as $N \rightarrow \infty$.

⁸Assuming the sequence of points is dense in Ω

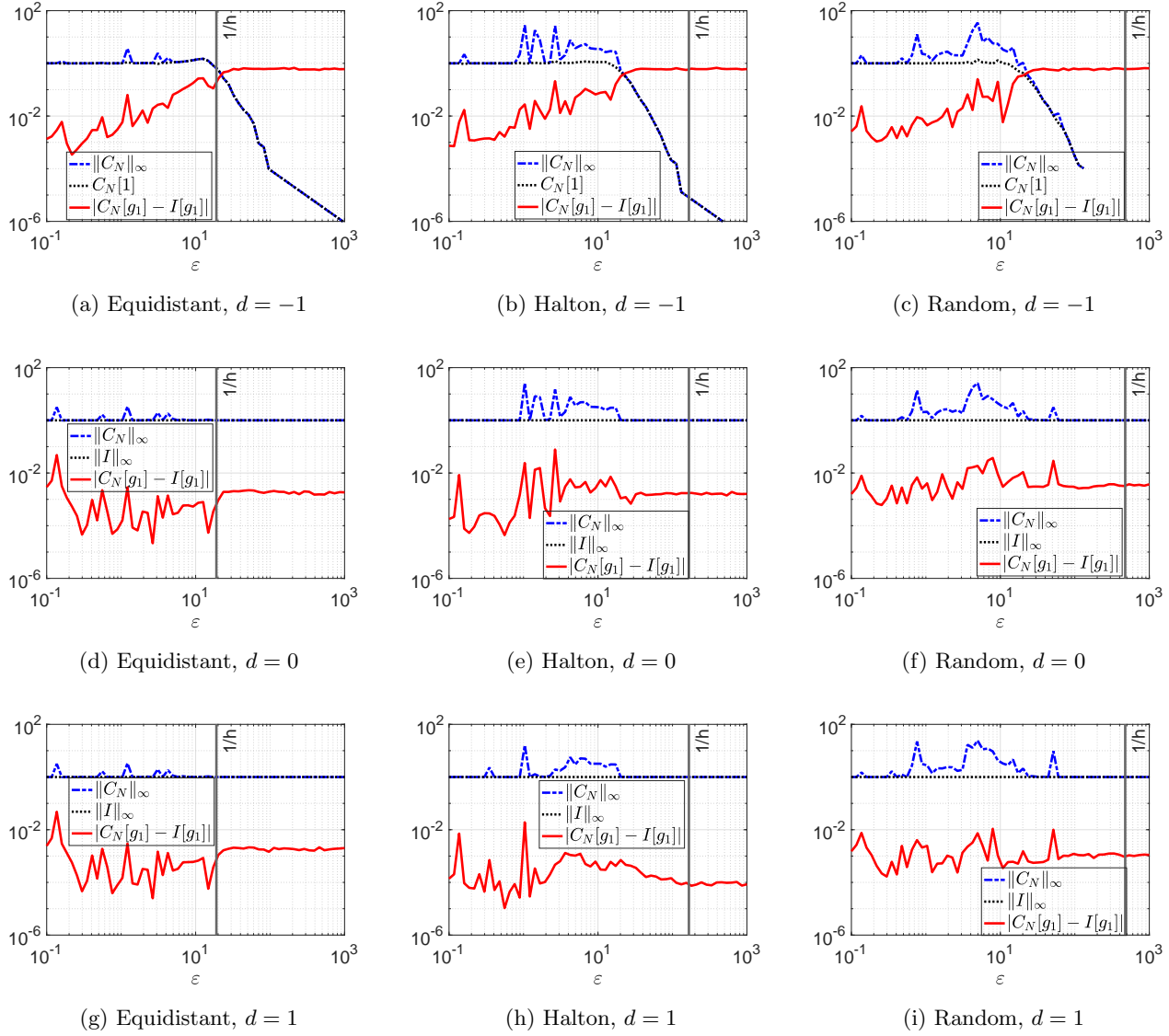


Figure 3: Error analysis for Wendland's compactly supported RBF $\varphi_{2,k}$ and the first Genz test function g_1 on $\Omega = [0, 1]^2$; see (7.1). In all cases, $N = 400$ data points (equidistant, Halton, or random) were considered. $1/h$ denotes the threshold above which the basis functions have nonoverlapping support.

Remark 7.1. If the RBF interpolant $s_{N,d}f$ converges to f in $L^1(\Omega)$ as $N \rightarrow \infty$, we get

$$|C_N[f] - I[f]| = |I[s_{N,d}f] - I[f]| \leq \int_{\Omega} |(s_{N,d}f)(\mathbf{x}) - f(\mathbf{x})| d\mathbf{x} \rightarrow 0, \quad N \rightarrow \infty,$$

and therefore $C_N[f] \rightarrow I[f]$ as $N \rightarrow \infty$. For convergence results of RBF interpolants, we refer to the monographs [12, 98, 27]. That said, we point out that the convergence of $s_{N,d}f$ to f depends on the area not covered by the supports. Let us denote the area that is covered by the supports by $\Omega_{\text{supp}(\varphi, X_N, \varepsilon)}$, then the area that is not covered by the supports is $\Omega \setminus \Omega_{\text{supp}(\varphi, X_N, \varepsilon)}$. A rough but simple lower bound for the $L^1(\Omega)$ -error of $s_{N,d}f$ and f is as follows. Note that the RBF interpolant is zero on $\Omega \setminus \Omega_{\text{supp}(\varphi, X_N, \varepsilon)}$

| | g_1 | | | g_4 | | |
|--------------------|------------|---------------|--------------------|------------|---------------|--------------------|
| | e_{\min} | ε | $\ C_N\ _{\infty}$ | e_{\min} | ε | $\ C_N\ _{\infty}$ |
| Equidistant Points | | | | | | |
| $d = 0$ | 2.2e-05 | 2.6e+00 | 1.0e+00 | 6.1e-05 | 2.6e+00 | 1.0e+00 |
| $d = 1$ | 2.2e-05 | 2.6e+00 | 1.0e+00 | 6.2e-05 | 2.6e+00 | 1.0e+00 |
| Halton Points | | | | | | |
| $d = 0$ | 4.7e-05 | 5.5e-01 | 1.0e+00 | 1.9e-05 | 5.5e-01 | 1.0e+00 |
| $d = 1$ | 1.1e-05 | 5.5e-01 | 1.0e+00 | 1.6e-05 | 5.5e-01 | 1.0e+00 |
| Random Points | | | | | | |
| $d = 0$ | 6.0e-04 | 2.5e-01 | 1.0e+00 | 1.6e-04 | 2.9e-01 | 1.0e+00 |
| $d = 1$ | 2.2e-04 | 4.0e-01 | 1.0e+00 | 1.7e-04 | 4.0e-01 | 1.0e+00 |

Table 2: Minimal errors, e_{\min} , for the first and fourth Genz test function, g_1 and g_4 , together with the corresponding shape parameter, ε , and stability measure, $\|C_N\|_{\infty}$. Wendland's compactly supported RBF with smoothness parameter $k = 1$ was used in all cases.

and thus

$$(7.2) \quad \int_{\Omega} |(s_{N,d}f)(\mathbf{x}) - f(\mathbf{x})| d\mathbf{x} \geq \int_{\Omega \setminus \Omega_{\text{supp}(\varphi, X_N, \varepsilon)}} |f(\mathbf{x})| d\mathbf{x},$$

where the right-hand side is the average absolute value of f in the area not covered by the supports. (7.2) indicates that convergence includes the rate with which “holes” go to zero.

In Figures 4 and 5, we relate the error in computing the integral of g_1 on $\Omega = [0, 1]^2$ to the portion of the domain that is not covered by the possibly overlapping supports of the Wendland functions. For equidistant points, the horizontal/vertical distance between adjacent points is (i.e. \mathbf{x}_{ij} and $\mathbf{x}_{(i\pm 1)j}$ or \mathbf{x}_{ij} and $\mathbf{x}_{i(j\pm 1)}$) is $1/(\sqrt{N} - 1)$, so as long as $\varepsilon > 2(\sqrt{N} - 1)$ the circles do not overlap and the total area that is not covered by the supports is given by

$$1 - \frac{\pi}{\varepsilon^2}(\sqrt{N} - 1)^2.$$

Once $\varepsilon \leq 2(\sqrt{N} - 1)$, the circles overlap, and the total area that is not covered by the supports becomes

$$1 - \frac{\pi}{\varepsilon^2}(\sqrt{N} - 1)^2 + \frac{2(\theta - \sin(\theta))}{\varepsilon^2}(\sqrt{N} - 1)^2,$$

where

$$\theta = 2\sin^{-1} \left(\frac{\sqrt{4(\sqrt{N} - 1)^2 - \varepsilon^2}}{2(\sqrt{N} - 1)} \right).$$

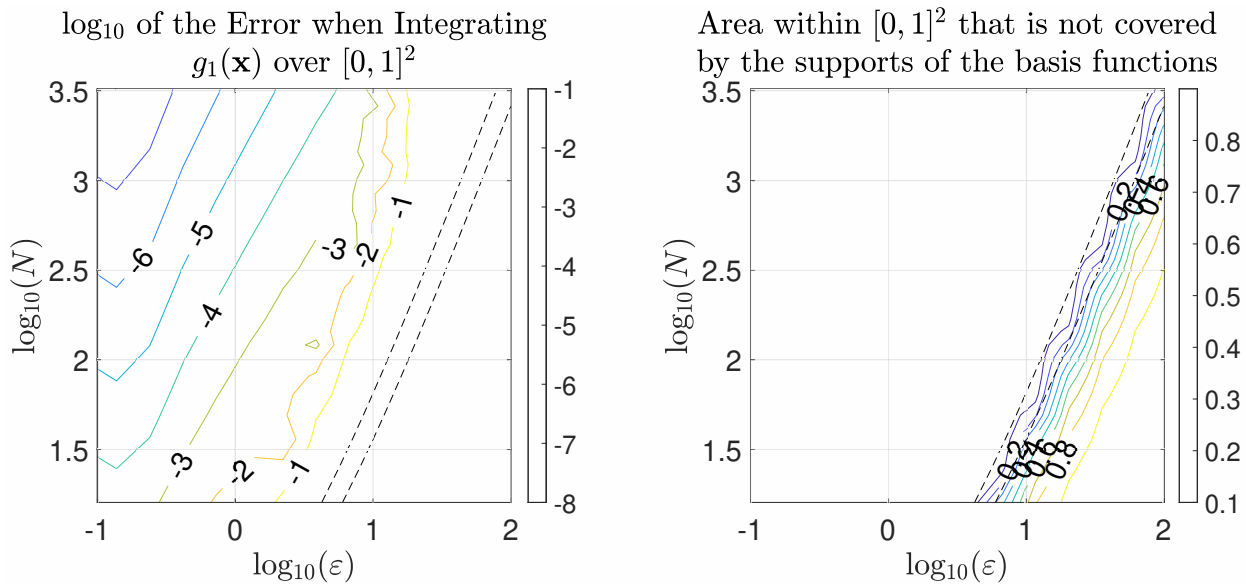


Figure 4: Error of $C_N[g_1]$ on $\Omega = [0, 1]^2$ and the area not covered by the supports of the Wendland functions for various N and ε when no constant is included in the RBF interpolant

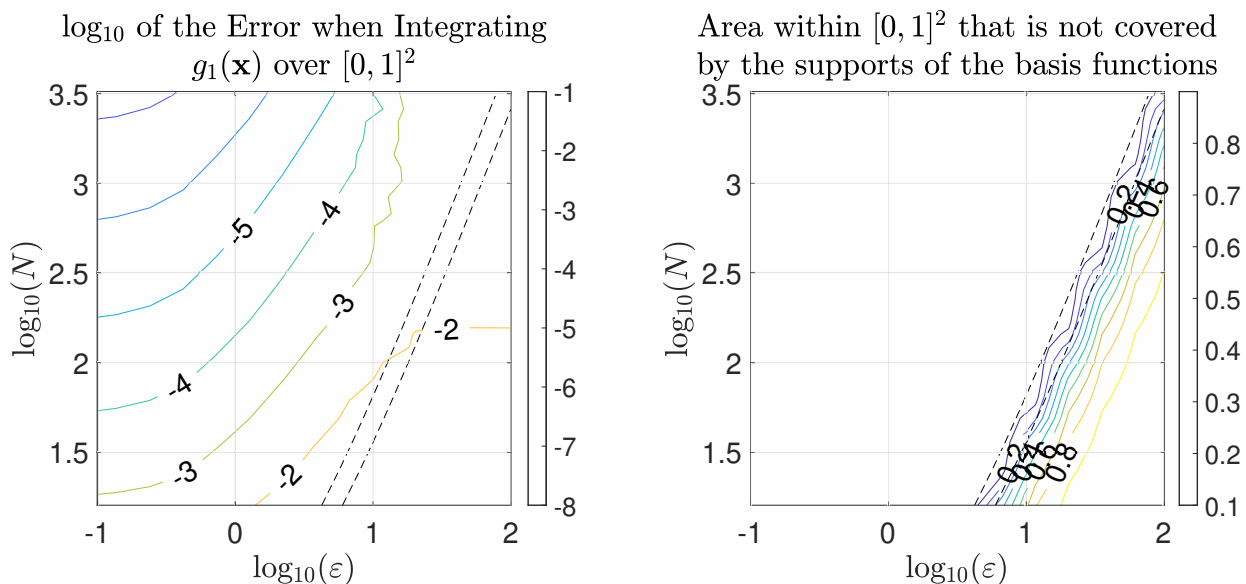


Figure 5: Error of $C_N[g_1]$ on $\Omega = [0, 1]^2$ and the area not covered by the supports of the Wendland functions for various N and ε when a constant is included in the RBF interpolant

Finally, when $\varepsilon \leq \sqrt{2}(\sqrt{N} - 1)$, the area that is not covered by the supports is 0. Figure 4 illustrates the error (left frame) and the area not covered by the supports (right frame) in this situation for various N and ε . The dashed lines represent the cases $\varepsilon = 2(\sqrt{N} - 1)$ and $\varepsilon = \sqrt{2}(\sqrt{N} - 1)$. On the other hand, Figure 5 illustrates the same test for an RBF interpolant that includes a constant. It demonstrates the improvement when the constant basis element covers the holes.

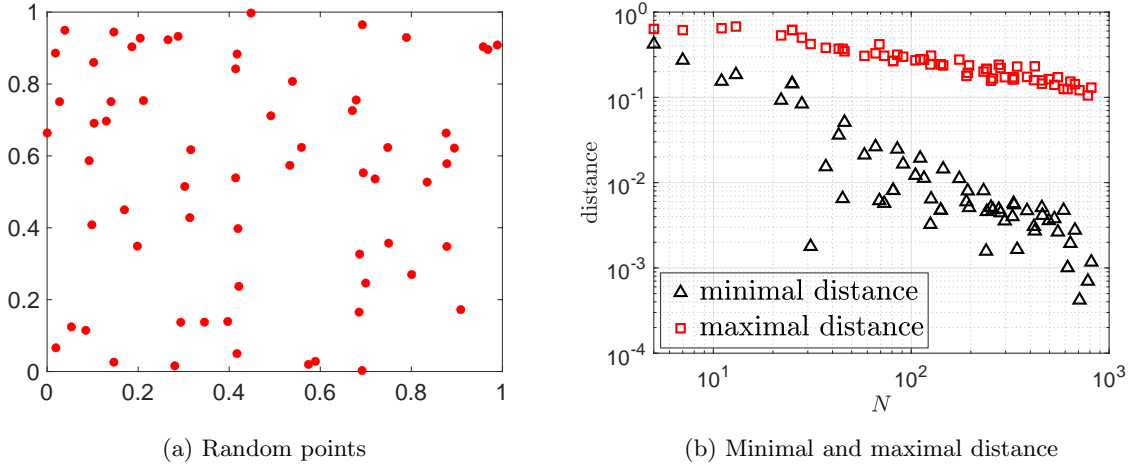


Figure 6: Random points and the corresponding minimal and maximal distance, (7.3) and (7.4). The minimal distance is the smallest distance between any two distinct points. The maximal distance is the largest distance between any point and the closest distinct point.

7.2. Stable LSRBF-QFs. We demonstrate that the least-squares approach discussed in §5 can stabilize RBF-QFs. We repeat that stable LSRBF-QF can be constructed for any RBF function space as long as we are willing to oversample, i. e., the number of data points used by the quadrature is larger than the dimension of the RBF function space. In other words, there are more data points than center points. Notably, oversampling was used in some recent works [89, 90, 41] to stabilize RBF methods for partial differential equations, and it would be of interest to combine this with LSRBF-QF in future works. Here, we demonstrate the possible advantage of LSRBF-QFs compared to interpolatory RBF-QFs (data and center points are the same) for the RBF function space spanned by a constant and the functions $\varphi(\varepsilon\|\mathbf{x} - \mathbf{y}_m\|)$ on $\Omega = [0, 1]^2$ using a Gaussian kernel $\varphi(r) = \exp(-r^2)$ and a constant (independent of the center and data points) shape parameter $\varepsilon = 0.8$. The center and data points, $\{\mathbf{y}_m\}_{m=1}^M$ and $\{\mathbf{x}_n\}_{n=1}^N$, are chosen as the first M and N elements of the same sequence of random points, respectively.

Figure 6a illustrates the first 64 random points from the sequence used in our tests. Figure 6b visualizes the minimal and maximal distance of the random data point set $X_N = \{\mathbf{x}_n\}_{n=1}^N$ for different values for N . We define the minimal distance of X_N , denoted by $h_{\min}(X_N)$, as the smallest distance between any two distinct points,

$$(7.3) \quad h_{\min}(X_N) = \min_{\mathbf{x}_n \in X_N} \min_{\mathbf{x}_m \in X_N \setminus \mathbf{x}_n} \|\mathbf{x}_m - \mathbf{x}_n\|_2.$$

At the same time, we define the maximal (filling) distance of X_N , denoted by $h_{\max}(X_N)$, as the largest distance between any point and the closest distinct point,

$$(7.4) \quad h_{\max}(X_N) = \max_{\mathbf{x}_n \in X_N} \min_{\mathbf{x}_m \in X_N \setminus \mathbf{x}_n} \|\mathbf{x}_m - \mathbf{x}_n\|_2.$$

Figure 7a provides the values of the stability measure for the interpolatory RBF-QF (“RBF”) and the stable LSRBF-QF (“LSRBF”). For the same center points (same RBF function space for which the quadrature is exact), the LSRBF-QF uses more data points to evaluate the integrand than the

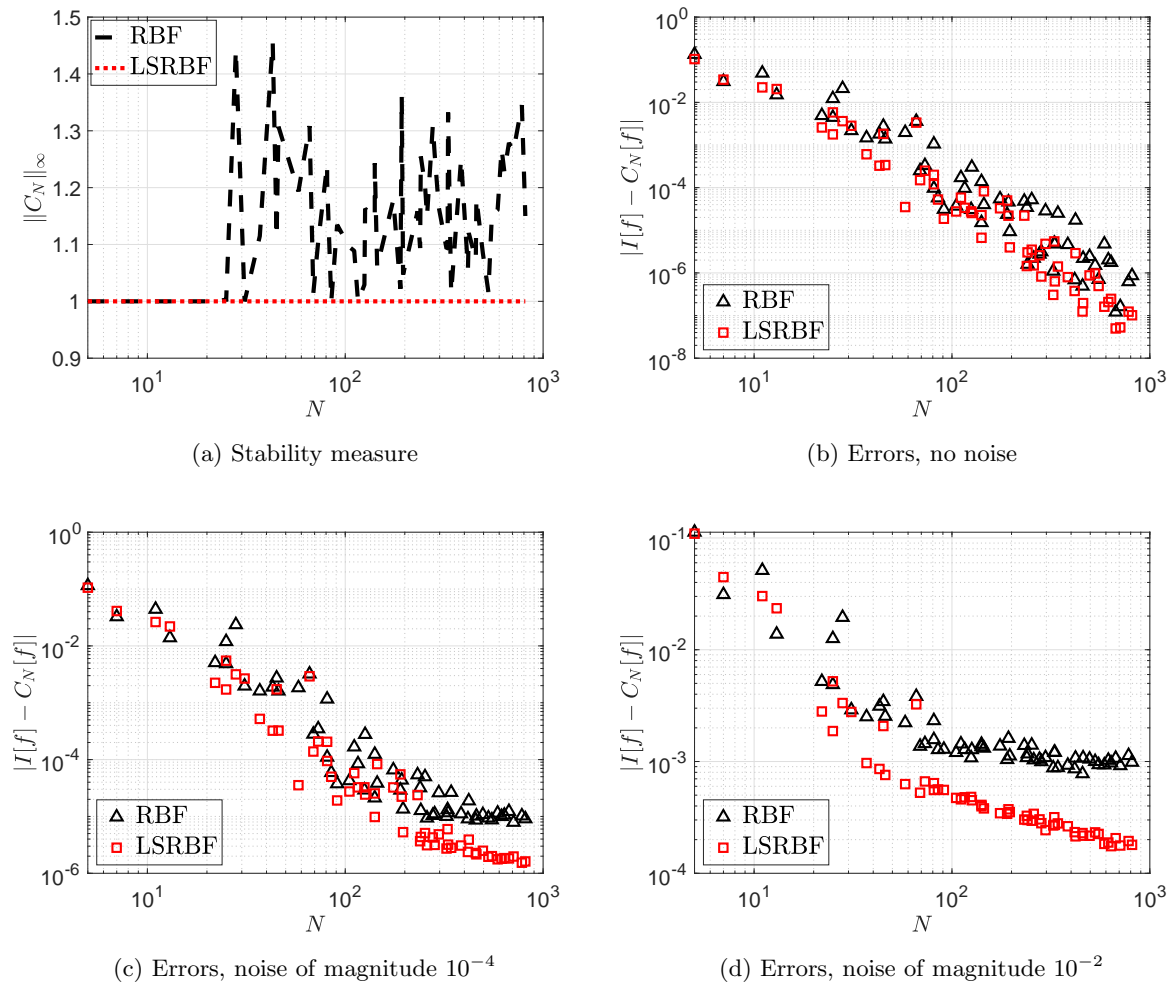


Figure 7: Stability measure and errors for Genz' first test function g_1 on $\Omega = [0, 1]^2$ with $\omega \equiv 1$ using an interpolatory RBF-QF and a stable LSRBF-QF. Random points and a Gaussian kernel with a constant shape parameter were used.

interpolatory RBF-QF. The other way around, for the same data points, the interpolatory RBF-QF is exact for a larger RBF function space than the LSRBF-QF. At the same time, the interpolatory RBF-QF is found to have a suboptimal stability measure (due to negative weights), which results in stability issues. In contrast, in all cases, the LSRBF-QF has an optimal stability measure (due to the weights being positive). Further, Figure 7b reports on the errors of the interpolatory RBF-QF and the stable LSRBF-QF on N random points applied to Genz' first test function g_1 on $\Omega = [0, 1]^2$ with $\omega \equiv 1$. In this example, both formulas perform similarly. In Figures 7c and 7d, we repeated this experiment but added uniformly distributed noise of magnitude 10^{-4} and 10^{-2} to the function values at the data points. The accuracy of the interpolatory RBF-QF deteriorates notably stronger than that of the LSRBF-QF in the presence of noise due to the improved stability of the latter. We made the same observation also for other point distributions and Genz test functions.

The LSRBF-QF having an optimal stability measure (being positive) for sufficiently large N can be explained by Corollary 5.2 since we are given a compact domain, a positive weight function, and

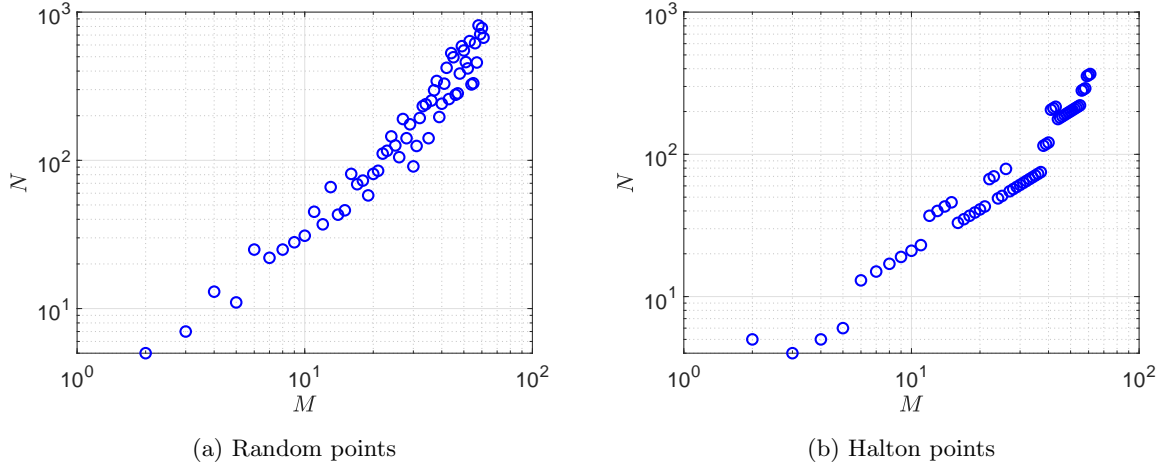


Figure 8: The smallest number of random/Halton data points, N , needed to find a positive LSRBF-QF that is exact for the RBF approximation space induced by the first M random/Halton center points.

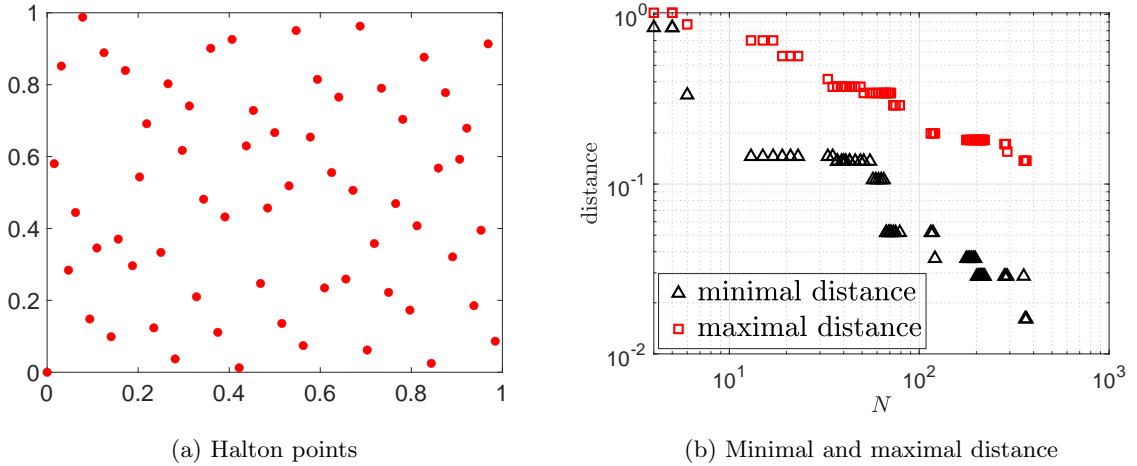


Figure 9: Halton points and the corresponding minimal and maximal distance, (7.3) and (7.4). The minimal distance is the smallest distance between any two distinct points. The maximal distance is the largest distance between any point and the closest distinct point.

a function space of continuous and bounded functions that contains constants. Figure 8 reports the smallest number of random/Halton data points N we needed to find a positive LSRBF-QF that is exact for the RBF approximation space induced by using the first M random/Halton points as centers. To also illustrate the semi-random Halton points, Figure 9 visualizes the first 64 Halton points and their minimal and maximal distance for an increasing number N . Considering the model “ $N = C \cdot M^s$ ” and performing a least-squares fit for the parameters C and s given the data illustrated in Figure 8 revealed the following: For random data and center points, we found $C \approx 2.1 \cdot 10^{-1}$ and $s \approx 1.9$. For Halton data and center points, we found $C \approx 4.9 \cdot 10^{-2}$ and $s \approx 2.1$. In both cases, we found N to be roughly linearly

proportional to the squared dimension of the approximation space for which the positive least-squares quadrature is exact. Similar ratios were also observed in [48, 42, 36, 35, 37, 16, 17, 66, 38]. It might be argued that the observed ratio between N and M is necessary for the LSRBF-QF to avoid inherent stability issues predicted by the ‘impossibility’ theorem proved in [74], which states that any procedure for approximating univariate functions from equally spaced samples that converges exponentially fast must also be exponentially ill-conditioned.

Finally, we address the convergence rate observed in Figure 7b. In theory, Gaussian RBF interpolants can converge almost exponentially fast⁹ in the $L^\infty(\Omega)$ with the maximal (filling) distance. For simplicity, we considered the model “ $|I[f] - C_N[f]| = \exp(-Ch_{\max}(X_N)^s)$ ” and performing a least-squares fit for the parameters C and s using the data presented in Figure 7b. For the interpolatory RBF-QF, we found $C \approx 2.0$ and $s \approx -1.1$. For the LSRBF-QF, we found $C \approx 1.8$ and $s \approx -1.3$. Both QFs converge roughly exponentially, with the LSRBF-QF converging slightly faster than the interpolatory RBF-QF, even in the noiseless case. A more general comment on the convergence of LSRBF-QFs is offered in Remark 7.2.

Remark 7.2 (Convergence of LSRBF-QF). Assume that the positive LSRBF-QF C_N on Ω is exact for all functions from the RBF approximation space $\mathcal{S}_{M,d}(\Omega)$ with $d \geq 0$. Due to C_N being positive and exact for constants, we have $\|C_N\|_\infty = \|I\|_\infty$ and the Lebesgue inequality (3.1) implies

$$|C_N[f] - I[f]| \leq 2\|I\|_\infty \left(\inf_{s \in \mathcal{S}_{M,d}(\Omega)} \|f - s\|_{L^\infty(\Omega)} \right)$$

for any continuous $f : \Omega \rightarrow \mathbb{R}$. Now consider a sequence of positive LSRBF-QFs $(C_N)_{N \in \mathbb{N}}$ with C_N being exact for $\mathcal{S}_{M,d}(\Omega)$ with $M = M(N)$. Assume that $\mathcal{S}_{M,d}(\Omega) \subset \mathcal{S}_{M+1,d}(\Omega)$ for all $M \in \mathbb{N}$ and that the given function f lies in $\bigcup_{M \in \mathbb{N}} \mathcal{S}_{M,d}(\Omega)$. Thus, if $M(N) \rightarrow \infty$ for $N \rightarrow \infty$, then $(C_N[f])_{N \in \mathbb{N}}$ converges to $I[f]$ as $N \rightarrow \infty$. Let us now assume that the ratio between M and N is of the form $N = \mathcal{O}(M^2)$, which we numerically observed to be true. The convergence rate of the LSRBF-QF for f is then the square root of the convergence rate of the best approximation of f from the sequence of approximation spaces $(\mathcal{S}_{M,d}(\Omega))_{N \in \mathbb{N}}$ for the $L^\infty(\Omega)$ -norm.

7.3. Polyharmonic splines. We end this section by providing a similar investigation for PHS. Again, the first and fourth Genz test functions on $\Omega = [0, 1]^2$ are considered. However, no shape parameter is involved for PHS, and we consider their stability and accuracy for an increasing number of Halton points. Figure 10 shows the results for the cubic ($\varphi(r) = r^3$) and quintic ($\varphi(r) = r^5$) PHS RBF. We either added no polynomials ($d = -1$) or polynomial terms of order $d = 0$ and $d = 1$. Figure 10 shows that all RBF-QFs converge while being stable or at least asymptotically stable, independent of the added polynomial term. In particular, we see that adding polynomial terms does not affect the asymptotic stability of the PHS RBF-QFs, per our results from §6. Finally, we see that the convergence rate of the RBF-QF depends on the kernel rather than being governed by the polynomial degree d . The added polynomial term reduces the error of the PHS RBF-QF but not the convergence rate. We observe second-order convergence for the cubic PHS RBF and third-order convergence for the quintic PHS RBF.¹⁰

⁹For a function from the appropriate native function space, the $L^\infty(\Omega)$ -error between the function and its RBF interpolant is in $\mathcal{O}(\exp(-C \log h_{\max}(X_N)/h_{\max}(X_N)))$; see [98].

¹⁰In Figure 10a the cubic PHS RBF-QF first shows third-order convergence before it then settles for second-order convergence. We believe that the observed initial third-order decrease in the error is a combination of the second-order approximation rate of the cubic PHS-RBF interpolant and the decreasing Lebesgue constant $\|C_N\|_\infty$ in (3.1). Once the QF is stable ($\|C_N\|_\infty = \|I\|_\infty$), the second-order approximation rate dominates the error of the QF, and we thus start to observe second-order convergence.

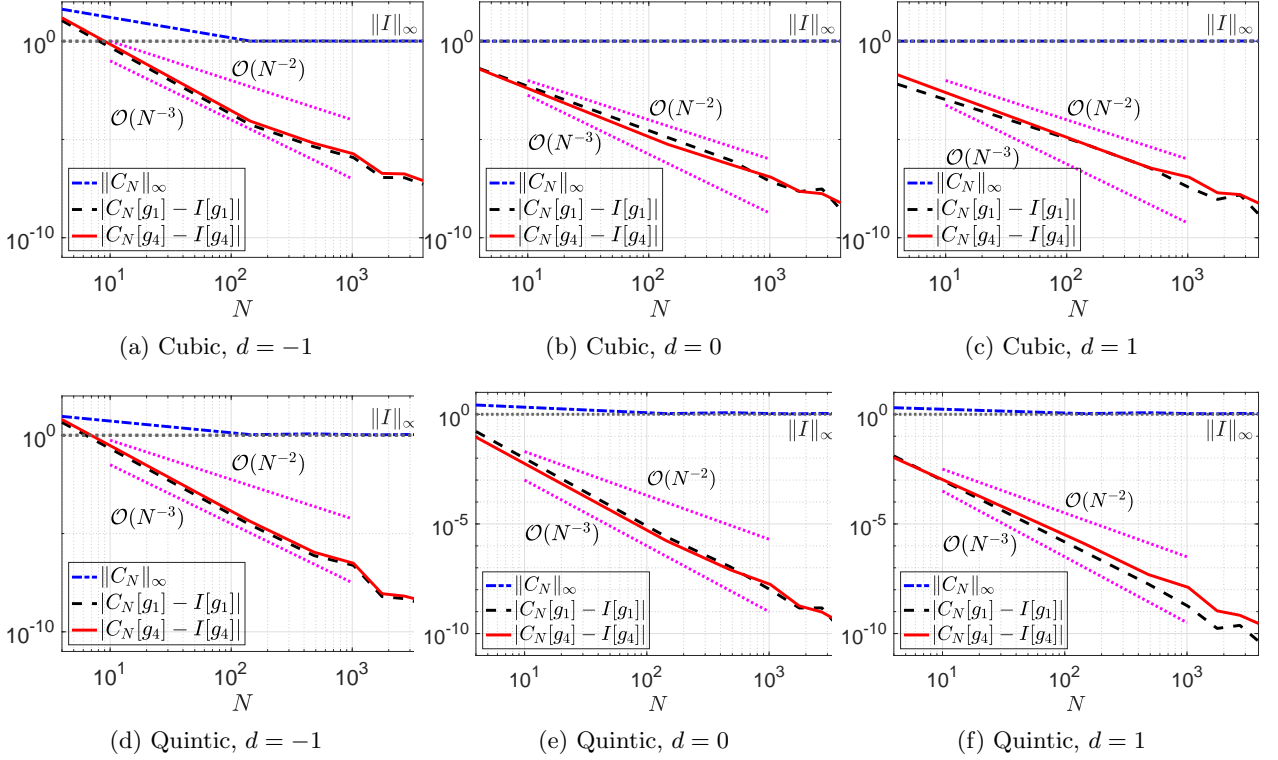


Figure 10: Error analysis for the cubic ($\varphi(r) = r^3$) and quintic ($\varphi(r) = r^5$) PHS RBF in two dimensions using Halton points. The first and fourth Genz test functions g_1, g_4 were considered on $\Omega = [0, 1]^2$; see (7.1).

8. Concluding thoughts. In this work, we investigated stability of RBF-QFs. We started by showing that stability of RBF-QFs can be connected to the famous Lebesgue constant of the underlying RBF interpolant. This indicates that RBF-QFs might benefit from low Lebesgue constants. Furthermore, stability was proven for RBF-QFs based on compactly supported RBFs under the assumption of a sufficiently large number of (equidistributed) data points and the shape parameter(s) lying above a certain threshold. Finally, we showed that under certain conditions, asymptotic stability of RBF-QFs is independent of polynomial terms included in RBF approximations. A series of numerical tests accompanied the above findings.

Acknowledgements. JG was supported by AFOSR #F9550-18-1-0316 and ONR #N00014-20-1-2595. We thank Toni Karvonen for pointing out the connection between RBF-QFs and Bayesian quadrature.

Appendix A. Moments.

Henceforth, we provide the moments for different RBFs. The one-dimensional case is discussed in §A.1, while two-dimensional moments are derived in §A.2.

A.1. One-dimensional moments. Let us consider the one-dimensional case of $\Omega = [a, b]$ and distinct data points $x_1, \dots, x_N \in [a, b]$.

A.1.1. Gaussian RBF. For $\varphi(r) = \exp(-\varepsilon^2 r^2)$, the moment of the translated Gaussian RBF,

$$(A.1) \quad m_n = m(\varepsilon, x_n, a, b) = \int_a^b \exp(-\varepsilon^2 |x - x_n|^2) dx,$$

is given by

$$m_n = \frac{\sqrt{\pi}}{2\varepsilon} [\operatorname{erf}(\varepsilon(b - x_n)) - \operatorname{erf}(\varepsilon(a - x_n))].$$

Here, $\operatorname{erf}(x) = 2/\sqrt{\pi} \int_0^x \exp(-t^2) dt$ denotes the usual *error function*, [73, Section 7.2].

A.1.2. Polyharmonic splines. For $\varphi(r) = r^k$ with odd $k \in \mathbb{N}$, the moment of the translated PHS,

$$m_n = m(x_n, a, b) = \int_a^b \varphi(x - x_n) dx,$$

is given by

$$m_n = \frac{1}{k+1} [(a - x_n)^{k+1} + (b - x_n)^{k+1}], \quad n = 1, 2, \dots, N.$$

For $\varphi(r) = r^k \log r$ with even $k \in \mathbb{N}$, on the other hand, we have

$$m_n = (x_n - a)^{k+1} \left[\frac{\log(x_n - a)}{k+1} - \frac{1}{(k+1)^2} \right] + (b - x_n)^{k+1} \left[\frac{\log(b - x_n)}{k+1} - \frac{1}{(k+1)^2} \right].$$

Note that for $x_n = a$ the first term is zero, while for $x_n = b$ the second term is zero.

A.2. Two-dimensional moments. Here, we consider the two-dimensional case, where the domain is given by a rectangular of the form $\Omega = [a, b] \times [c, d]$.

A.2.1. Gaussian RBF. For $\varphi(r) = \exp(-\varepsilon^2 r^2)$, the two-dimensional moments can be written as products of one-dimensional moments. In fact, we have

$$\int_a^b \int_c^d \exp(-\varepsilon^2 \|(x - x_n, y - y_n)\|_2^2) = m(\varepsilon, x_n, a, b) \cdot m(\varepsilon, y_n, c, d).$$

Here, the multiplicands on the right-hand side are the one-dimensional moments from (A.1).

A.2.2. Polyharmonic splines and other RBFs. If it is not possible to trace the two-dimensional moments back to the one-dimensional ones, we are in need of another approach. This is, for instance, the case for PHS. We start by noting that for a data points $(x_n, y_n) \in [a, b] \times [c, d]$ the corresponding moment can be rewritten as follows:

$$m(x_n, y_n) = \int_a^b \int_c^d \varphi(\|(x - x_n, y - y_n)^T\|_2) dy dx = \int_{\tilde{a}}^{\tilde{b}} \int_{\tilde{c}}^{\tilde{d}} \varphi(\|(x, y)^T\|_2) dy dx$$

with translated boundaries $\tilde{a} = a - x_n$, $\tilde{b} = b - x_n$, $\tilde{c} = c - y_n$, and $\tilde{d} = d - y_n$. We are not aware of an explicit formula for such integrals for most popular RBFs readily available from the literature. That said, such formulas were derived in [78, 80, 79] (also see [95, Chapter 2.3]) for the integral of φ over a *right triangle* with vertices $(0, 0)^T$, $(\alpha, 0)^T$, and $(\alpha, \beta)^T$. Assuming $\tilde{a} < 0 < \tilde{b}$ and $\tilde{c} < 0 < \tilde{d}$, we therefore partition the shifted domain $\tilde{\Omega} = [\tilde{a}, \tilde{b}] \times [\tilde{c}, \tilde{d}]$ into eight right triangles. Denoting the

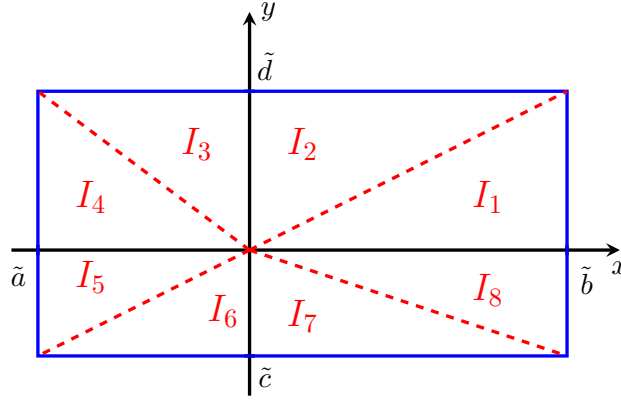


Figure 11: Illustration of how the moments can be computed on a rectangle in two dimensions

corresponding integrals by I_1, \dots, I_8 , the moment $m(x_n, y_n)$ correspond to the sum of these integrals. The procedure is illustrated in Figure 11.

The special cases where one (or two) of the edges of the rectangle align with one of the axes can be treated similarly. However, in this case, a smaller subset of the triangles is considered. We leave the details to the reader, and note the following formula for the weights:

$$\begin{aligned} m(x_n, y_n) = & \left[1 - \delta_0(\tilde{b}\tilde{d})\right] (I_1 + I_2) + \left[1 - \delta_0(\tilde{a}\tilde{d})\right] (I_3 + I_4) \\ & + \left[1 - \delta_0(\tilde{a}\tilde{c})\right] (I_5 + I_6) + \left[1 - \delta_0(\tilde{b}\tilde{c})\right] (I_7 + I_8) \end{aligned}$$

Here, δ_0 denotes the usual Kronecker delta defined as $\delta_0(x) = 1$ if $x = 0$ and $\delta_0(x) = 0$ if $x \neq 0$. The above formula holds for general \tilde{a} , \tilde{b} , \tilde{c} , and \tilde{d} . Note that all the right triangles can be rotated or mirrored in a way that yields a corresponding integral of the form

$$(A.2) \quad I_{\text{ref}}(\alpha, \beta) = \int_0^\alpha \int_0^{\frac{\beta}{\alpha}x} \varphi(\|(x, y)^T\|_2) dy dx.$$

More precisely, we have

$$\begin{aligned} I_1 &= I_{\text{ref}}(\tilde{b}, \tilde{d}), & I_2 &= I_{\text{ref}}(\tilde{d}, \tilde{b}), & I_3 &= I_{\text{ref}}(\tilde{d}, -\tilde{a}), & I_4 &= I_{\text{ref}}(-\tilde{a}, \tilde{d}), \\ I_5 &= I_{\text{ref}}(-\tilde{a}, -\tilde{c}), & I_6 &= I_{\text{ref}}(-\tilde{c}, -\tilde{a}), & I_7 &= I_{\text{ref}}(-\tilde{c}, \tilde{b}), & I_8 &= I_{\text{ref}}(\tilde{b}, -\tilde{c}). \end{aligned}$$

Finally, explicit formulas of the reference integral $I_{\text{ref}}(\alpha, \beta)$ over the right triangle with vertices $(0, 0)^T$, $(\alpha, 0)^T$, and $(\alpha, \beta)^T$ for some PHS can be found in Table 3. Similar formulas are also available, for instance, for Gaussian, multiquadric and inverse multiquadric RBFs.

We note that the approach presented above is similar to the one in [85], where the domain $\Omega = [-1, 1]^2$ was considered. Later, the same authors extended their findings to simple polygons [84] using the Gauss–Green theorem. Also see the recent work [86], addressing polygonal regions that may be nonconvex or even multiply connected, and references therein. It would be of interest to see if these approaches also carry over to computing products of RBFs corresponding to different centers or products of RBFs and their partial derivatives, again corresponding to different centers. Such integrals occur as elements of mass and stiffness matrices in numerical PDEs. In particular, they are desired to construct linearly energy stable (global) RBF methods for hyperbolic conservation laws [35, 39, 40].

| $\varphi(r)$ | $I_{\text{ref}}(\alpha, \beta)$ |
|--------------|--------------------------------------------------------------------------------------------------------------------------------------------------------------------------------------------|
| $r^2 \log r$ | $\frac{\alpha}{144} \left[24\alpha^3 \arctan(\beta/\alpha) + 6\beta(3\alpha^2 + \beta^2) \log(\alpha^2 + \beta^2) - 33\alpha^2\beta - 7\beta^3 \right]$ |
| r^3 | $\frac{\alpha}{40} \left[3\alpha^4 \operatorname{arcsinh}(\beta/\alpha) + \beta(5\alpha^2 + 2\beta^2) \sqrt{\alpha^2 + \beta^2} \right]$ |
| r^5 | $\frac{\alpha}{336} \left[15\alpha^6 \operatorname{arcsinh}(\beta/\alpha) + \beta(33\alpha^4 + 26\alpha^2\beta^2 + 8\beta^4) \sqrt{\alpha^2 + \beta^2} \right]$ |
| r^7 | $\frac{\alpha}{3346} \left[105\alpha^8 \operatorname{arcsinh}(\beta/\alpha) + \beta(279\alpha^6 + 326\alpha^4\beta^2 + 200\alpha^2\beta^4 + 48\beta^6) \sqrt{\alpha^2 + \beta^2} \right]$ |

Table 3: The reference integral $I_{\text{ref}}(\alpha, \beta)$ —see (A.2)—for some PHS

REFERENCES

- [1] W. F. AMES, *Numerical Methods for Partial Differential Equations*, Academic Press, 2014.
- [2] I. AZIZ, W. KHAN, ET AL., *Numerical integration of multi-dimensional highly oscillatory, gentle oscillatory and non-oscillatory integrands based on wavelets and radial basis functions*, *Engineering Analysis with Boundary Elements*, 36 (2012), pp. 1284–1295.
- [3] I. BABUŠKA AND J. M. MELENK, *The partition of unity method*, *International Journal for Numerical Methods in Engineering*, 40 (1997), pp. 727–758.
- [4] V. BAYONA, *Comparison of moving least squares and RBF+poly for interpolation and derivative approximation*, *Journal of Scientific Computing*, 81 (2019), pp. 486–512.
- [5] V. BAYONA, *An insight into RBF-FD approximations augmented with polynomials*, *Computers & Mathematics with Applications*, 77 (2019), pp. 2337–2353.
- [6] L. BOS, M. CALIARI, S. DE MARCHI, M. VIANELLO, AND Y. XU, *Bivariate Lagrange interpolation at the Padua points: the generating curve approach*, *Journal of Approximation Theory*, 143 (2006), pp. 15–25.
- [7] L. BOS AND S. DE MARCHI, *Univariate radial basis functions with compact support cardinal functions*, *East Journal on Approximations*, 14 (2008), p. 69.
- [8] L. BOS, S. DE MARCHI, M. VIANELLO, AND Y. XU, *Bivariate Lagrange interpolation at the Padua points: the ideal theory approach*, *Numerische Mathematik*, 108 (2007), pp. 43–57.
- [9] H. BRASS AND K. PETRAS, *Quadrature Theory: The Theory of Numerical Integration on a Compact Interval*, no. 178 in *Mathematical Surveys and Monographs*, AMS, 2011.
- [10] F.-X. BRIOL, C. J. OATES, M. GIROLAMI, M. A. OSBORNE, AND D. SEJDINOVIC, *Probabilistic integration: A role in statistical computation?*, *Statistical Science*, 34 (2019), pp. 1–22.
- [11] L. BRUTMAN, *Lebesgue functions for polynomial interpolation—a survey*, *Annals of Numerical Mathematics*, 4 (1996), pp. 111–128.
- [12] M. D. BUHMANN, *Radial basis functions*, *Acta Numerica*, 9 (2000), pp. 1–38.
- [13] M. D. BUHMANN, *Radial Basis Functions: Theory and Implementations*, vol. 12, Cambridge University Press, 2003.
- [14] R. E. CAFLISCH, *Monte Carlo and quasi-Monte Carlo methods*, *Acta Numerica*, 1998 (1998), pp. 1–49.
- [15] R. CAVORETTO, A. DE ROSSI, A. SOMMARIVA, AND M. VIANELLO, *RBF-CUB: A numerical package for near-optimal meshless cubature on general polygons*, *Applied Mathematics Letters*, 125 (2022), p. 107704.
- [16] A. COHEN, M. A. DAVENPORT, AND D. LEVIATAN, *On the stability and accuracy of least squares approximations*, *Foundations of Computational Mathematics*, 13 (2013), pp. 819–834.
- [17] A. COHEN AND G. MIGLIORATI, *Optimal weighted least-squares methods*, *The SMAI Journal of Computational Mathematics*, 3 (2017), pp. 181–203.
- [18] R. COOLS, *Constructing cubature formulae: The science behind the art*, *Acta Numerica*, 6 (1997), pp. 1–54.
- [19] R. COOLS, *An encyclopaedia of cubature formulas*, *Journal of Complexity*, 19 (2003), pp. 445–453.
- [20] R. COOLS, I. MYSOVSKIKH, AND H. SCHMID, *Cubature formulae and orthogonal polynomials*, *Journal of Computational and Applied Mathematics*, 127 (2001), pp. 121–152.
- [21] P. J. DAVIS AND P. RABINOWITZ, *Methods of Numerical Integration*, Courier Corporation, 2007.
- [22] S. DE MARCHI, *On optimal center locations for radial basis function interpolation: computational aspects*, *Rend. Splines Radial Basis Functions and Applications*, 61 (2003), pp. 343–358.
- [23] S. DE MARCHI AND R. SCHABACK, *Stability of kernel-based interpolation*, *Advances in Computational Mathematics*, 32 (2010), pp. 155–161.
- [24] J. DICK, F. Y. KUO, AND I. H. SLOAN, *High-dimensional integration: The quasi-Monte Carlo way*, *Acta Numerica*,

- 22 (2013), p. 133.
- [25] H. ENGELS, *Numerical Quadrature and Cubature*, Academic Press, 1980.
- [26] G. E. FASSHAUER, *Solving partial differential equations by collocation with radial basis functions*, in Proceedings of Chamonix, vol. 1997, Vanderbilt University Press Nashville, TN, 1996, pp. 1–8.
- [27] G. E. FASSHAUER, *Meshfree Approximation Methods with MATLAB*, vol. 6, World Scientific, 2007.
- [28] N. FLYER, G. A. BARNETT, AND L. J. WICKER, *Enhancing finite differences with radial basis functions: experiments on the Navier–Stokes equations*, Journal of Computational Physics, 316 (2016), pp. 39–62.
- [29] G. B. FOLLAND, *How to integrate a polynomial over a sphere*, The American Mathematical Monthly, 108 (2001), pp. 446–448.
- [30] B. FORNBERG AND N. FLYER, *A Primer on Radial Basis Functions With Applications to the Geosciences*, SIAM, 2015.
- [31] B. FORNBERG AND N. FLYER, *Solving PDEs with radial basis functions*, Acta Numerica, 24 (2015), pp. 215–258.
- [32] E. FUSELIER, T. HANGELBROEK, F. J. NARCOWICH, J. D. WARD, AND G. B. WRIGHT, *Kernel based quadrature on spheres and other homogeneous spaces*, Numerische Mathematik, 127 (2014), pp. 57–92.
- [33] A. GENZ, *Testing multidimensional integration routines*, in Proc. of International Conference on Tools, Methods and Languages for Scientific and Engineering Computation, 1984, pp. 81–94.
- [34] P. GLASSERMAN, *Monte Carlo Methods in Financial Engineering*, vol. 53, Springer Science & Business Media, 2013.
- [35] J. GLAUBITZ, *Shock Capturing and High-Order Methods for Hyperbolic Conservation Laws*, Logos Verlag Berlin GmbH, 2020.
- [36] J. GLAUBITZ, *Stable high order quadrature rules for scattered data and general weight functions*, SIAM Journal on Numerical Analysis, 58 (2020), pp. 2144–2164.
- [37] J. GLAUBITZ, *Stable high-order cubature formulas for experimental data*, Journal of Computational Physics, (2021), p. 110693.
- [38] J. GLAUBITZ, *Construction and application of provable positive and exact cubature formulas*, IMA Journal of Numerical Analysis, (2022), <https://doi.org/10.1093/imanum/drac017>.
- [39] J. GLAUBITZ AND A. GELB, *Stabilizing radial basis function methods for conservation laws using weakly enforced boundary conditions*, Journal of Scientific Computing, 87 (2021), pp. 1–29.
- [40] J. GLAUBITZ, E. LE MELEDO, AND P. ÖFFNER, *Towards stable radial basis function methods for linear advection problems*, Computers & Mathematics with Applications, 85 (2021), pp. 84–97.
- [41] J. GLAUBITZ, J. NORDSTRÖM, AND P. ÖFFNER, *Energy-stable global radial basis function methods on summation-by-parts form*, arXiv preprint arXiv:2204.03291, (2022).
- [42] J. GLAUBITZ AND P. ÖFFNER, *Stable discretisations of high-order discontinuous Galerkin methods on equidistant and scattered points*, Applied Numerical Mathematics, 151 (2020), pp. 98–118.
- [43] S. HABER, *Numerical evaluation of multiple integrals*, SIAM Review, 12 (1970), pp. 481–526.
- [44] J. H. HALTON, *On the efficiency of certain quasi-random sequences of points in evaluating multi-dimensional integrals*, Numerische Mathematik, 2 (1960), pp. 84–90.
- [45] R. L. HARDY, *Multiquadric equations of topography and other irregular surfaces*, Journal of Geophysical Research, 76 (1971), pp. 1905–1915.
- [46] J. S. HESTHAVEN AND T. WARBURTON, *Nodal Discontinuous Galerkin Methods: Algorithms, Analysis, and Applications*, Springer Science & Business Media, 2007.
- [47] E. HLAWKA, *Funktionen von beschränkter Variation in der Theorie der Gleichverteilung*, Ann. Mat. Pura Appl., 54 (1961), pp. 325–333.
- [48] D. HUYBRECHS, *Stable high-order quadrature rules with equidistant points*, Journal of Computational and Applied Mathematics, 231 (2009), pp. 933–947.
- [49] B. A. IBRAHIMOGLU, *Lebesgue functions and Lebesgue constants in polynomial interpolation*, Journal of Inequalities and Applications, 2016 (2016), pp. 1–15.
- [50] A. ISKE, *On the approximation order and numerical stability of local Lagrange interpolation by polyharmonic splines*, in Modern Developments in Multivariate Approximation, Springer, 2003, pp. 153–165.
- [51] A. ISKE, *Radial basis functions: basics, advanced topics and meshfree methods for transport problems*, Rend. Sem. Mat. Univ. Pol. Torino, 61 (2003), pp. 247–285.
- [52] A. ISKE, *Scattered data approximation by positive definite kernel functions*, Rend. Sem. Mat. Univ. Pol. Torino, 69 (2011), pp. 217–246.
- [53] A. ISKE AND T. SONAR, *On the structure of function spaces in optimal recovery of point functionals for ENO-schemes by radial basis functions*, Numerische Mathematik, 74 (1996), pp. 177–201.
- [54] E. KANSA AND Y. HON, *Circumventing the ill-conditioning problem with multiquadric radial basis functions: Applications to elliptic partial differential equations*, Computers and Mathematics with Applications, 39 (2000), pp. 123–138.

- [55] E. J. KANSA, *Multiquadrics—a scattered data approximation scheme with applications to computational fluid-dynamics—ii Solutions to parabolic, hyperbolic and elliptic partial differential equations*, Computers & Mathematics with Applications, 19 (1990), pp. 147–161.
- [56] T. KARVONEN, M. KANAGAWA, AND S. SÄRKKÄ, *On the positivity and magnitudes of Bayesian quadrature weights*, Statistics and Computing, 29 (2019), pp. 1317–1333.
- [57] A. R. KROMMER AND C. W. UEBERHUBER, *Computational Integration*, SIAM, 1998.
- [58] V. I. KRYLOV AND A. H. STROUD, *Approximate Calculation of Integrals*, Courier Corporation, 2006.
- [59] L. KUIPERS AND H. NIEDERREITER, *Uniform Distribution of Sequences*, Courier Corporation, 2012.
- [60] E. LARSSON AND B. FORNBERG, *A numerical study of some radial basis function based solution methods for elliptic PDEs*, Computers & Mathematics with Applications, 46 (2003), pp. 891–902.
- [61] J. B. LASSERRE, *Simple formula for integration of polynomials on a simplex*, BIT Numerical Mathematics, 61 (2021), pp. 523–533.
- [62] B. F. MANLY, *Randomization, Bootstrap and Monte Carlo Methods in Biology*, vol. 70, CRC Press, 2006.
- [63] J. C. MAXWELL, *On approximate multiple integration between limits of summation*, in Proc. Cambridge Philos. Soc., vol. 3, 1877, pp. 39–47.
- [64] B. MEHRI AND S. JOKAR, *Lebesgue function for multivariate interpolation by radial basis functions*, Applied Mathematics and Computation, 187 (2007), pp. 306–314.
- [65] C. A. MICCHELLI AND T. J. RIVLIN, *A survey of optimal recovery*, Optimal Estimation in Approximation Theory, (1977), pp. 1–54.
- [66] G. MIGLIORATI AND F. NOBILE, *Stable high-order randomized cubature formulae in arbitrary dimension*, Journal of Approximation Theory, 275 (2022), p. 105706.
- [67] T. P. MINKA, *Deriving quadrature rules from Gaussian processes*, tech. report, Technical report, Statistics Department, Carnegie Mellon University, 2000.
- [68] K. P. MURPHY, *Machine Learning: A Probabilistic Perspective*, MIT Press, 2012.
- [69] I. MYSOVSKIKH, *The approximation of multiple integrals by using interpolatory cubature formulae*, in Quantitative Approximation, Elsevier, 1980, pp. 217–243.
- [70] I. P. MYSOVSKIKH, *Cubature formulae that are exact for trigonometric polynomials*, TW Reports, (2001). Edited by R. Cools and H.J. Schmid.
- [71] H. NIEDERREITER, *Random Number Generation and Quasi-Monte Carlo Methods*, SIAM, 1992.
- [72] A. O’HAGAN, *Bayes-hermite quadrature*, Journal of Statistical Planning and Inference, 29 (1991), pp. 245–260.
- [73] F. W. J. OLVER, A. B. OLDE DAALHUIS, D. W. LOZIER, B. I. SCHNEIDER, R. F. BOISVERT, C. W. CLARK, B. R. MILLER, B. V. SAUNDERS, H. S. COHL, AND M. A. MCCLAIN, *NIST Digital Library of Mathematical Functions*. Release 1.1.1, March 15, 2021, 2021, <http://dlmf.nist.gov/>.
- [74] R. B. PLATTE, L. N. TREFETHEN, AND A. B. KUIJLAARS, *Impossibility of fast stable approximation of analytic functions from equispaced samples*, SIAM Review, 53 (2011), pp. 308–318.
- [75] A. PUNZI, A. SOMMARIVA, AND M. VIANELLO, *Meshless cubature over the disk using thin-plate splines*, Journal of Computational and Applied Mathematics, 221 (2008), pp. 430–436.
- [76] A. QUARTERONI AND A. VALLI, *Numerical Approximation of Partial Differential Equations*, vol. 23, Springer Science & Business Media, 2008.
- [77] J. A. REEGER, *Approximate integrals over the volume of the ball*, Journal of Scientific Computing, 83 (2020), p. 45.
- [78] J. A. REEGER AND B. FORNBERG, *Numerical quadrature over the surface of a sphere*, Studies in Applied Mathematics, 137 (2016), pp. 174–188.
- [79] J. A. REEGER AND B. FORNBERG, *Numerical quadrature over smooth surfaces with boundaries*, Journal of Computational Physics, 355 (2018), pp. 176–190.
- [80] J. A. REEGER, B. FORNBERG, AND M. L. WATTS, *Numerical quadrature over smooth, closed surfaces*, Proceedings of the Royal Society A: Mathematical, Physical and Engineering Sciences, 472 (2016), p. 20160401.
- [81] W. RUDIN, *Real and Complex Analysis*, McGraw-Hill Education, 1987.
- [82] V. SHANKAR, *The overlapped radial basis function-finite difference (RBF-FD) method: A generalization of RBF-FD*, Journal of Computational Physics, 342 (2017), pp. 211–228.
- [83] C. SHU AND Y. WU, *Integrated radial basis functions-based differential quadrature method and its performance*, International Journal for Numerical Methods in Fluids, 53 (2007), pp. 969–984.
- [84] A. SOMMARIVA AND M. VIANELLO, *Meshless cubature by Green’s formula*, Applied Mathematics and Computation, 183 (2006), pp. 1098–1107.
- [85] A. SOMMARIVA AND M. VIANELLO, *Numerical cubature on scattered data by radial basis functions*, Computing, 76 (2006), p. 295.
- [86] A. SOMMARIVA AND M. VIANELLO, *RBF moment computation and meshless cubature on general polygonal regions*, Applied Mathematics and Computation, 409 (2021), p. 126375.

- [87] A. SOMMARIVA AND R. WOMERSLEY, *Integration by rbf over the sphere*, Applied Mathematics Report AMR05/17, University of New South Wales, (2005).
- [88] A. H. STROUD, *Approximate Calculation of Multiple Integrals*, Prentice-Hall, 1971.
- [89] I. TOMINEC, E. LARSSON, AND A. HERYUDONO, *A least squares radial basis function finite difference method with improved stability properties*, SIAM Journal on Scientific Computing, 43 (2021), pp. A1441–A1471.
- [90] I. TOMINEC, M. NAZAROV, AND E. LARSSON, *Stability estimates for radial basis function methods applied to time-dependent hyperbolic PDEs*, arXiv preprint arXiv:2110.14548, (2021).
- [91] L. N. TREFETHEN, *Cubature, approximation, and isotropy in the hypercube*, SIAM Review, 59 (2017), pp. 469–491.
- [92] L. N. TREFETHEN, *Approximation Theory and Approximation Practice, Extended Edition*, SIAM, 2019.
- [93] L. N. TREFETHEN, *Exactness of quadrature formulas*, arXiv preprint arXiv:2101.09501, (2021).
- [94] L. VAN DEN BOS, B. SANDERSE, AND W. BIERBOOMS, *Adaptive sampling-based quadrature rules for efficient Bayesian prediction*, Journal of Computational Physics, (2020), p. 109537.
- [95] M. L. WATTS, *Radial basis function based quadrature over smooth surfaces*, 2016, <https://scholar.ait.edu/etd/249>. Theses and Dissertations.
- [96] H. WENDLAND, *Piecewise polynomial, positive definite and compactly supported radial functions of minimal degree*, Advances in Computational Mathematics, 4 (1995), pp. 389–396.
- [97] H. WENDLAND, *Fast evaluation of radial basis functions: Methods based on partition of unity*, in Approximation Theory X: Wavelets, Splines, and Applications, Citeseer, 2002.
- [98] H. WENDLAND, *Scattered Data Approximation*, vol. 17, Cambridge University Press, 2004.
- [99] H. WEYL, *Über die Gleichverteilung von Zahlen mod. Eins*, Mathematische Annalen, 77 (1916), pp. 313–352.